THE
EMBO
JOURNAL

TRANSPARENT
PROCESS

α-Synuclein stimulation of monoamine oxidase-B and legumain protease mediates the pathology of Parkinson's disease

Seong Su Kang[1], Eun Hee Ahn[1], Zhentao Zhang[1,2], Xia Liu[1], Fredric P Manfredsson[3] (iD), Ivette M Sandoval[3] (iD), Susov Dhakal[4], P Michael Iuvone[4], Xuebing Cao[5,*] (iD) & Keqiang Ye[1,6,**] (iD)

Abstract

Dopaminergic neurodegeneration in Parkinson's disease (PD) is associated with abnormal dopamine metabolism by MAO-B (monoamine oxidase-B) and intracellular α-Synuclein (α-Syn) aggregates, called the Lewy body. However, the molecular relationship between α-Syn and MAO-B remains unclear. Here, we show that α-Syn directly binds to MAO-B and stimulates its enzymatic activity, which triggers AEP (asparagine endopeptidase; legumain) activation and subsequent α-Syn cleavage at N103, leading to dopaminergic neurodegeneration. Interestingly, the dopamine metabolite, DOPAL, strongly activates AEP, and the N103 fragment of α-Syn binds and activates MAO-B. Accordingly, overexpression of AEP in SNCA transgenic mice elicits α-Syn N103 cleavage and accelerates PD pathogenesis, and inhibition of MAO-B by Rasagiline diminishes α-Syn-mediated PD pathology and motor dysfunction. Moreover, virally mediated expression of α-Syn N103 induces PD pathogenesis in wild-type, but not MAO-B-null mice. Our findings thus support that AEP-mediated cleavage of α-Syn at N103 is required for the association and activation of MAO-B, mediating PD pathogenesis.

Introduction

Parkinson's disease (PD) is characterized by selective degeneration of dopaminergic neurons in the substantia nigra pars compacta (SNc) and the resultant decrease in dopaminergic innervation of the striatum. The etiology of PD appears to be multifactorial, involving both genetic and environmental components (Lee & Trojanowski, 2006). Most cases of PD are sporadic, with unknown disease etiology. However, several familial forms of PD have been described. One such form arises due to mutations or multiplications of the gene encoding α-Synuclein (α-Syn; SNCA), an abundant presynaptic protein (Polymeropoulos et al, 1997; Kruger et al, 1998). Misfolded α-Syn is the principal component of Lewy pathology, and α-syn thus plays a key role in the etiopathogenesis of PD, as the disorder is characterized neuropathologically by the accumulation of intraneuronal protein aggregates (Lewy bodies and Lewy neurites).

Aging and exposure to neurotoxins are considered the most prominent risk factors for the development of idiopathic PD. In addition to familial and sporadic PD, toxic forms of PD are known. The best characterized toxin that causes PD is 1-methyl-4-phenyl-1,2,3,6-tetrahydropyridine (MPTP; Langston & Ballard, 1983; Przedborski & Jackson-Lewis, 1998). Parkinsonism induced by MPTP is clinically indistinguishable from idiopathic PD. Furthermore, experimental treatment of animals with MPTP leads to neuronal cell loss in the SNc and to a marked reduction in the neostriatal concentrations of dopamine and its metabolites similar to PD. After MPTP is administered to animals, it is transported to the brain where it is converted by monoamine oxidase-B (MAO-B) into 1-methyl-4-phenylpyridinium (MPP$^+$; Heikkila et al, 1984). Interestingly, there is an increased localization of α-Syn into nigral soma with aging (Jellinger, 2004; Chu & Kordower, 2007) and increased levels of α-syn are seen in MPTP-treated animals (Kowall et al, 2000; Vila et al, 2000). Nonetheless, α-Syn is not an obligatory component by which MPTP damages dopaminergic neurons, although at least in some genetic backgrounds, deletion of α-Syn can protect mice from MPTP toxicity (Schluter et al, 2003; Klivenyi et al, 2006; Thomas et al, 2011).

MAO-A and MAO-B are the major enzymes that catalyze the oxidative deamination of monoamine neurotransmitters such as

1 Department of Pathology and Laboratory Medicine, Emory University School of Medicine, Atlanta, GA, USA
2 Department of Neurology, Renmin Hospital of Wuhan University, Wuhan, China
3 Translational Science and Molecular Medicine, College of Human Medicine, Michigan State University, Grand Rapids, MI, USA
4 Department of Ophthalmology and Pharmacology, Emory University School of Medicine, Atlanta, GA, USA
5 Department of Neurology, Union Hospital, Tongji Medical College, Huazhong University of Science and Technology, Wuhan, China
6 Translational Center for Stem Cell Research, Department of Regenerative Medicine, Tongji Hospital, Tongji University School of Medicine, Shanghai, China
*Corresponding author. Tel: +86 150 7140 5700; E-mail: caoxuebing@126.com
**Corresponding author. Tel: +1 404 712 2814; E-mail: kye@emory.edu

dopamine (DA), noradrenaline, and serotonin in the central and peripheral nervous systems. MAOs are involved in depression and in a number of neurodegenerative disorders such as PD. Age-related augmentation of MAO-B expression is associated with increases in free radical damage and reactive oxygen species (ROS; Saura *et al*, 1994; Mahy *et al*, 2000). This increase in free radicals and ROS via an age-dependent increase in MAO-B expression leads to a decrease in neuronal mitochondrial function, reduction in viability of SNc neurons, and ultimately neurodegeneration (Koppula *et al*, 2012) and the resultant motor impairment. For instance, genetic elevation of MAO levels in dopaminergic PC12 cells results in increased free radical damage and sensitivity to MPTP. Moreover, increased expression of MAO-B results in enhanced neurite degeneration in methamphetamine-treated PC12 cells (Wei *et al*, 1996, 1997). Monoamine oxidase-B is an outer mitochondrial membrane protein that oxidizes arylalkylamine neurotransmitters and has been a valuable drug target for many neurological disorders (Shih, 2004). Monoamine oxidase-B inhibitors such as L-(-)-deprenyl (Selegiline) and Rasagiline are effective for the treatment of PD. Since MAO-B is mainly localized in glial cells, increases in astrocytic MAO-B expression, mimicking that which occurs with aging and in neurodegenerative disease, in a doxycycline (dox)-inducible transgenic mouse model evoke neuropathological similarities to what is observed in the human parkinsonian brain (Mallajosyula *et al*, 2008; Siddiqui *et al*, 2011). Notably, the dox-inducible astrocytic MAO-B transgenic mouse displays similar age-related behavioral and neuropathological features to other models of PD, and could serve as a useful tool to study PD pathophysiology and for the evaluation of therapeutic interventions (Lieu *et al*, 2013). On the other hand, MAO-B KO mice are resistant to MPTP (Grimsby *et al*, 1997), and inhibition of MAO-B attenuates MPTP neurotoxicity (Chen *et al*, 2002).

Recently, we demonstrated that asparagine endopeptidase (AEP, LGMN) is upregulated and activated in the brain during aging, and cleaves both APP and Tau. Importantly, AEP is selectively activated in human AD brains as compared to healthy controls, causing amyloid plaque and neurofibrillary tangle (NFT) formation, mediating AD pathogenesis (Zhang *et al*, 2014, 2015). Blockade of AEP via small-molecule inhibition confers therapeutic efficacy in various AD mouse models (Zhang *et al*, 2017b). Most recently, we reported that AEP cleaves human α-Syn at N103 in an age-dependent manner, promoting α-Syn aggregation and enhancing neurotoxicity, leading to dopaminergic neuronal loss and motor impairments in PD. AEP is also highly activated in human PD brains. Overexpression of the AEP-cleaved α-Syn 1-103 fragment in substantia nigra induces both dopaminergic neuronal loss and motor defects. By contrast, inhibition of α-Synuclein (wild-type and A53T) cleavage by AEP eliminates its pathologic activity. Hence, AEP might play a critical role in mediating the pathogenesis of PD by cleaving α-Syn (Zhang *et al*, 2017a). In the current study, we show that α-Syn selectively binds MAO-B and elevates its enzymatic activity, and the AEP-cleaved α-Syn N103 fragment exhibits the strongest binding affinity and catalytic activity toward MAO-B. In alignment with these findings, AEP is required for MPTP-triggered MAO-B activation. On the other hand, the MAO-B enzymatic DA metabolite, DOPAL, activates AEP and triggers α-Syn N103 cleavage. Accordingly, AEP overexpression facilitates the onset of PD pathologies in SNCA transgenic mice, and α-Syn fails to induce PD pathogenesis in the presence of MAO-B inhibitor or in MAO-B-null mice.

Results

α-Synuclein binds MAO-B

Mounting evidence demonstrates that oxidative stress, DA metabolism, and α-Syn are tightly interconnected events in PD pathogenesis. α-Syn and DA metabolism work synergistically to trigger neurodegeneration (Conway *et al*, 2001; Hasegawa *et al*, 2006). To test whether α-Syn directly interacts with DA oxidative enzymes, we performed a GST pull-down assay by cotransfecting mammalian GST-tagged (mGST) α-Syn with Myc-MAOs into HEK293 cells, and found that α-Syn selectively bound to MAO-B but not MAO-A (Fig 1A). A mapping assay revealed that the N-terminal 1–103 truncate of α-Syn exhibited the strongest binding affinity, whereas the a.a. 65–140 fragment exhibited a weak interaction with MAO-B (Fig 1B). Aggregated α-Syn exhibits a specific phosphorylation pattern, and α-Syn mutations are causative in familial forms of PD. A co-immunoprecipitation assay showed that phosphorylation mutants of a.a. S129 or Y125 did not affect its association with MAO-B. Moreover, neither the A53T nor the A30P mutants displayed different binding activities toward MAO-B as compared to wild-type α-Syn (Fig 1C). Noticeably, MPTP treatment enhanced the specific interaction between endogenous α-Syn and MAO-B in samples collected from mouse SN. Again, there was no binding by α-Syn to MAO-A or MFN1, another mitochondrial protein. As expected, MPTP selectively augmented MAO-B but not MAO-A protein levels. Both α-Syn and its S129 phosphorylation levels were elevated following MPTP treatment (Fig 1D). Interestingly, we made similar observations with human PD brain samples. It is worth noting that both MAO-B and α-Syn protein levels were higher in PD patients than healthy controls. We have recently reported that AEP, an age-dependent cysteine protease, is highly activated in human PD brains and cleaves α-Syn at N103, promoting its aggregation and neurotoxicity (Zhang *et al*, 2017a). Accordingly, α-Syn N103 was much more abundant in PD brains than controls (Fig 1E). Although MAO-B is mainly localized in the outer membrane of mitochondrion in astrocytes, it also occurs in neurons as well (Shih, 2004). Immunofluorescent staining showed that MAO-B was distributed in TH-positive dopaminergic neurons. The middle TH-positive neuron with white arrow demonstrated the clear localization of MAO-B in neuron (Fig 1F). Its abundance was much higher in PD brains than in healthy controls, co-localizing with elevated α-Syn, and MAO-B was localized in the Lewy bodies of PD patient brains as well (Fig 1G). To further explore the subcellular distribution of α-Syn and MAO-B, we conducted immunofluorescent staining on the SH-SY5Y dopaminergic cell line after treatment with MPP$^+$ (1-methyl-4-phenylpyridinium), a neurotoxic metabolite of MPTP produced by MAO-B. MPP$^+$ treatment greatly amplified the protein levels of both α-Syn and MAO-B in SH-SY5Y cells (Fig EV1A), in addition to the truncated α-Syn N103, which colocalized with MAO-B. This colocalization occurred in mitochondria, which was verified by co-labeling with the mitochondrial biomarker TOMM20 (Fig EV1B and C). Thus, α-Syn selectively binds to MAO-B at the mitochondria.

α-Synuclein stimulates MAO-B enzymatic activity

To assess the biological effect of α-Syn binding to MAO-B, we performed an *in vitro* MAO-B enzymatic assay in the presence of
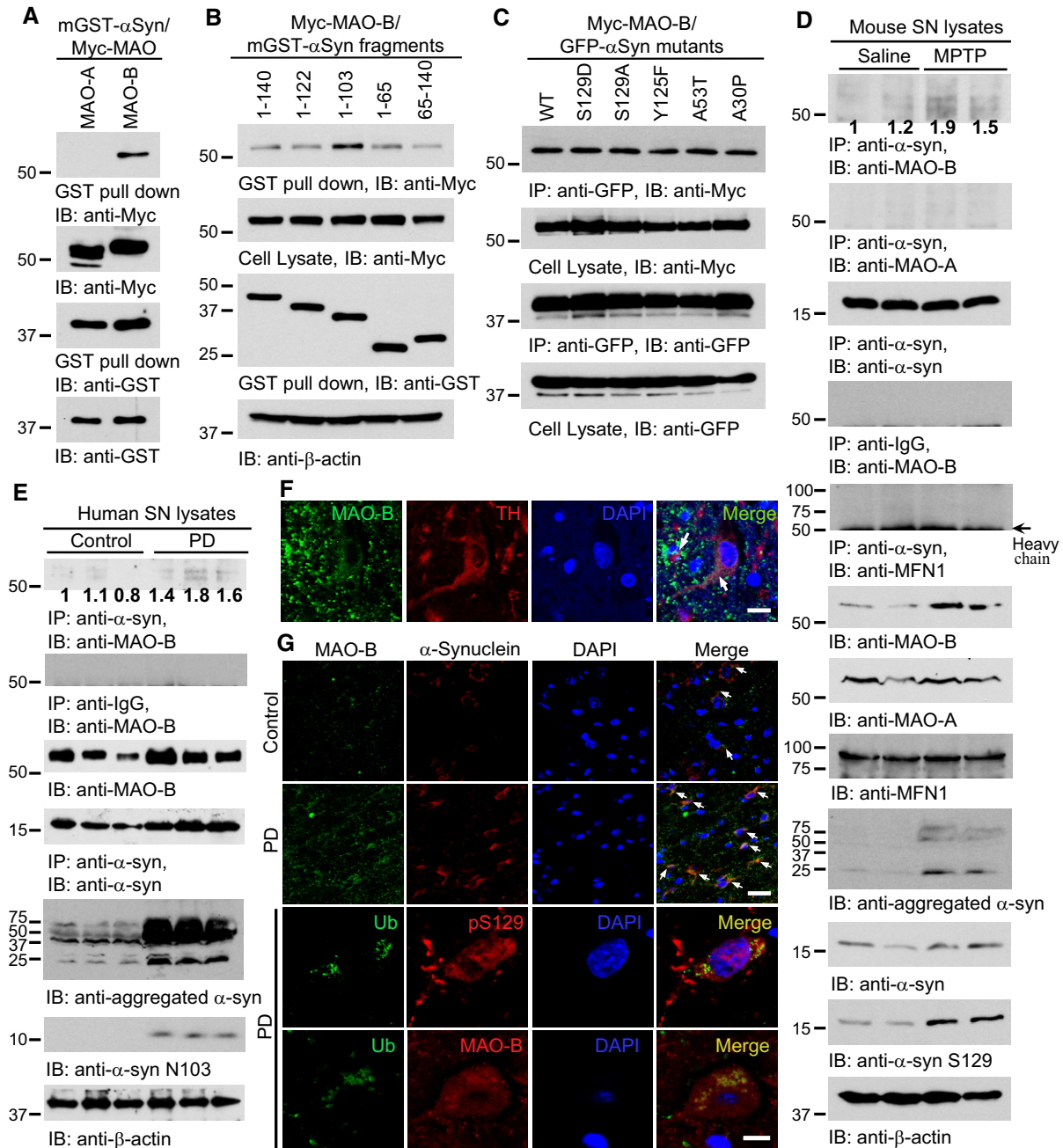
Figure 1. α-Synuclein selectively interacts with MAO-B.

A α-Syn specifically binds MAO-B. GST pull-down assay was conducted from HEK293 cells co-transfected with mammalian GST-α-Syn and Myc-MAO-A or MAO-B.

B Mapping α-Syn binding domain to MAO-B. α-Syn 1–103 fragment displayed the strongest binding affinity toward MAO-B. Different mGST-tagged α-Syn truncates were co-transfected with Myc-MAO-B into HEK293 cells. A GST pull-down assay was performed, and co-precipitated proteins were analyzed by immunoblotting with anti-Myc (upper panels).

C α-Syn mutants bind to MAO-B. Various GFP-α-Syn mutants were co-transfected with Myc-MAO-B. A GST pull-down assay was performed, and co-precipitated proteins were analyzed by immunoblotting with anti-Myc (upper panels).

D MPTP (30 mg/kg) enhances the interaction between α-Syn and MAO-B. Immunoprecipitation in substantia nigra tissue of MPTP-treated mice was performed with anti-α-Syn, and the precipitated proteins were analyzed by immunoblotting with anti-MAO-B. Densitometric quantification normalized by each α-Syn immunoblot was marked in the image (top panel). Cell lysates were probed with various antibodies (4th to bottom panels).

E α-Syn interacts with MAO-B in human PD patient brains. Brain lysates from PD patients were immunoprecipitated with anti-α-Syn, and the precipitated proteins were analyzed by immunoblotting with anti-MAO-B. Densitometric quantification normalized by each α-Syn immunoblot was marked in the image.

F MAO-B localizes to TH-positive dopaminergic neurons in substantia nigra of human brain. Scale bar is 20 μm.

G MAO-B co-localizes with α-Syn in dopaminergic cells of PD patients. Immunofluorescent signals of anti-MAO-B (Green) and α-Syn (Red) were increased in PD brain sections. MAO-B was also localized in the Lewy bodies of PD patient brain. The nuclei were stained with DAPI. Scale bars are 50 μm (2nd panel) and 20 μm (4th panel). Arrows show co-localized cells of MAO-B and α-synuclein.
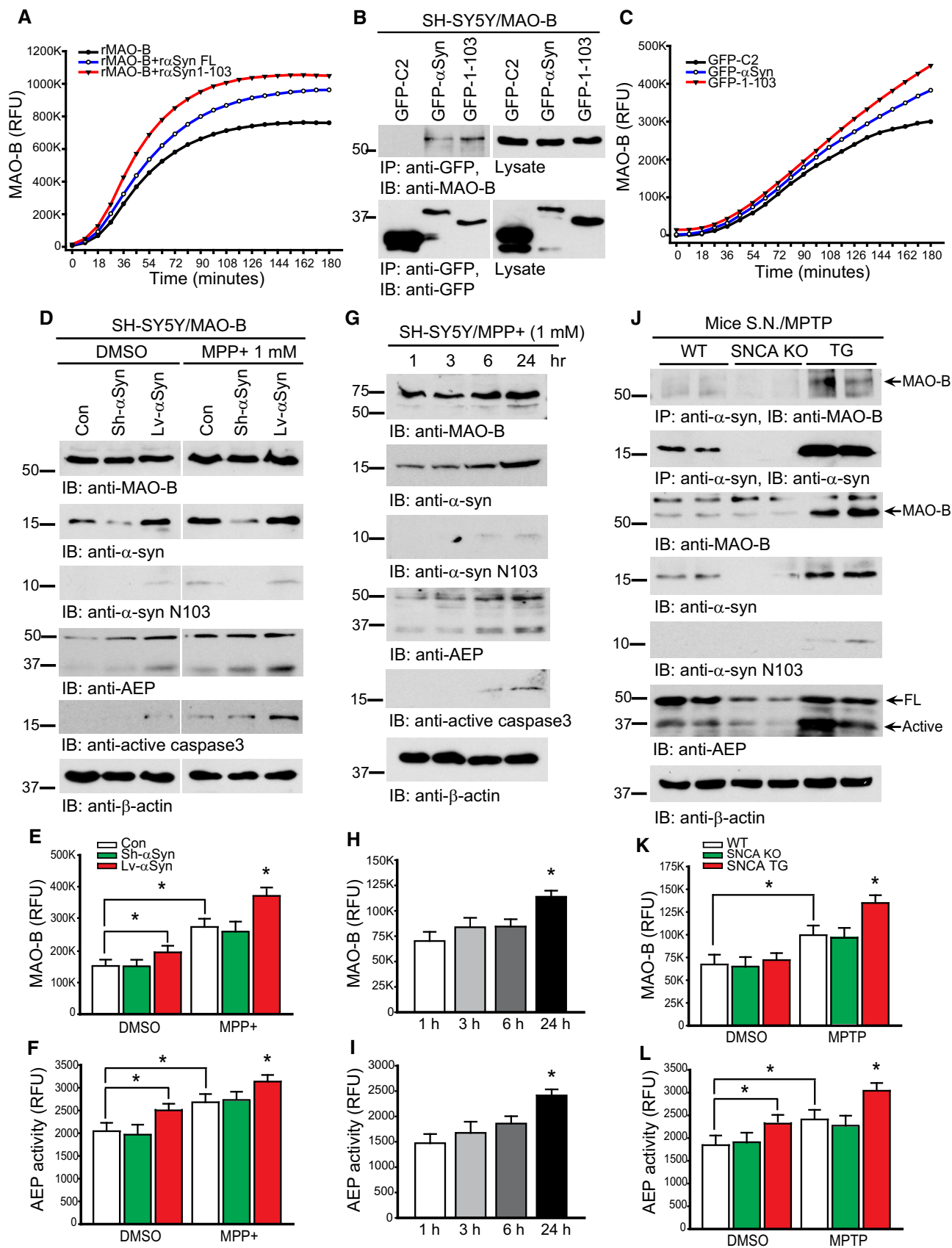
Figure 2.

Figure 2. α-Synuclein catalyzes MAO-B enzymatic activity.

A   α-Syn increases MAO-B enzymatic activity. Recombinant MAO-B proteins were incubated with purified α-Syn or α-Syn 1–103 fragment proteins, and an MAO-B enzymatic assay was conducted.

B, C   α-Syn activates MAO-B in intact cells. MAO-B was transfected with GFP-C2, GFP- α-Syn, or GFP-1–103 in SH-SY5Y cells. Transfected cell lysates were immunoprecipitated with anti-GFP, and the precipitated proteins were analyzed by immunoblotting with anti-MAO-B (B). Cell lysates were analyzed by a MAO-B enzymatic assay (C).

D   Sh-α-Syn or lenti-α-Syn was infected into SH-SY5Y cells and MAO-B was transfected, then followed by MPP$^+$ (1 mM) treatment for 24 h. Immunoblotting was conducted by various antibodies including anti-MAO-B.

E, F   Knockdown of α-Syn inhibits α-Syn-induced MAO-B and AEP activities. Cell lysates were analyzed by MAO-B and AEP enzymatic assays.

G   MPP$^+$ increases MAO-B expression in a time-dependent manner. SH-SY5Y cells were treated with MPP$^+$ (1 mM) for 1, 3, 6, or 24 h, and cell lysates were immunoblotted by various antibodies.

H, I   MAO-B and AEP enzymatic assays showed that MPP$^+$ enhanced their activity at 24 h.

J   SNCA TG mice treated with MPTP (30 mg/kg) enhance the interaction between α-Syn and MAO-B. Immunoprecipitation of substantia nigra tissue of MPTP-treated WT, SNCA KO, or SNCA TG mice was performed with anti-α-Syn, and the precipitated proteins were analyzed by immunoblotting with anti-MAO-B (top panel). Cell lysates were probed with various antibodies (2nd to bottom panels). FL, the full-length band of AEP. Active, active band related to AEP activity.

K, L   MPTP activates AEP and MAO-B in SNCA transgenic mice. MAO-B and AEP enzymatic assays showed that their activities were increased in SNCA TG mice compared to WT or SNCA KO mice, after administration of MPTP.

Data information: Data are shown as mean ± SEM. *N* = 3 each group. *P < 0.05.

purified recombinant α-Syn or its truncated N103 fragment. We found that α-Syn enhanced the enzymatic activity of MAO-B, and the N103 fragment displayed even more pronounced stimulatory effect on MAO-B activity (Fig 2A). The same observation was made with the co-transfection of MAO-B and GFP-tagged α-Syn in SH-SY5Y cells. Again, a higher degree of α-Syn N103 associated with MAO-B than full-length α-Syn, and the stimulatory effect on MAO-B enzymatic activity correlated with this binding affinity (Fig 2B and C). Both A53T and A30P mutants exhibited similar MAO-B stimulatory activity as wild-type α-Syn, fitting with their comparable binding effect on MAO-B. S129 or Y125 phosphorylation of α-Syn did not affect the stimulatory effect on MAO-B activity (Fig EV2A and B). To investigate whether α-Syn is required for MAO-B enzymatic activity triggered by MPP$^+$, we knocked down endogenous α-Syn in MAO-B-transfected SH-SY5Y cells using siRNA or overexpressed α-Syn using lentivirus, followed by MPP$^+$ stimulation. As expected, both α-Syn overexpression and MPP$^+$ increased MAO-B activity. However, the maximal effect was observed in α-Syn-overexpressing cells treated with MPP$^+$. These events were tightly associated with AEP upregulation and activation of its protease activity, and α-Syn N103 cleavage. In contrast, reducing α-Syn did not reduce either AEP or MAO-B activity (Fig 2D–F). A kinetic analysis revealed that MPP$^+$ increased endogenous MAO-B, α-Syn, and AEP protein levels in SH-SY5Y cells in a time-dependent manner, in concordance with MAO-B and AEP enzymatic activity. Again, the α-Syn N103 fragment was temporally elevated by MPP$^+$ (Fig 2G–I). Conceivably, MPP$^+$ treatment increases AEP levels and protease activity triggering proteolytic cleavage of α-Syn at N103, which subsequently catalyzes the increase in MAO-B enzymatic activity. To test whether the increase in MAO enzymatic activity is MAO-B specific, not MAO-A, we employed clorgyline (MAO-A inhibitor) and pargyline (MAO-B inhibitor) in the enzymatic assay. MAO-A activity inhibited by MAO-B inhibitor (pargyline) was not changed, whereas MAO-B activity using clorgyline was activated by MPP$^+$ treatment (Fig EV2C and D). Similarly, in the real-time PCR using specific PCR primers of MAO-A and MAO-B, we confirmed that only MAO-B, not MAO-A was increased by MPP$^+$ treatment (Fig EV2E and F). When tested *in vivo* in MPTP-treated SNCA transgenic or knockout (KO) mice, as we expected, the upregulated α-Syn exhibited a strong interaction with augmented MAO-B in nigral tissue, with a much stronger effect in transgenic mice as compared to wild-type mice. By contrast,

there was no interaction in SNCA KO mice. Once again, MPTP treatment elevated mature and active AEP in SNCA transgenic mice to a higher degree than that seen in wild-type mice, with SNCA KO mice exhibiting the lowest levels. α-Syn N103 levels closely paired with the concentrations of active AEP (Fig 2J), and both MAO-B and AEP enzymatic activity correlated with their corresponding protein levels in most cases (Fig 2K and L). Thus, MPTP upregulates the expression level of α-Syn, AEP, and MAO-B, and AEP-cleaved α-Syn N103 may subsequently catalyze MAO-B enzymatic activity.

AEP cleavage of α-Synuclein regulates its stimulatory activity toward MAO-B

To explore the potential role of AEP in mediating MPP$^+$-triggered MAO-B activity, we co-transfected MAO-B into SH-SY5Y cells with wild-type AEP or its dominant-negative C189S mutant, followed by MPP$^+$ treatment. In the presence of wild-type AEP but not the C189S mutant, α-Syn was prominently cleaved into N103. MPP$^+$ treatment greatly increased α-Syn protein levels, and its proteolytic cleavage was also enhanced with wild-type AEP as compared to control, while expression of the C189S mutant completely blocked α-Syn N103 cleavage (Fig 3A). MAO-B and AEP enzymatic activity showed a similar pattern which corresponded with α-Syn N103 levels (Fig 3B and C). To further assess the role of AEP in MPP$^+$-triggered MAO-B enzymatic activity, we reduced endogenous AEP expression using RNAi. As a result, the MPP$^+$-induced increase in AEP was repressed by its siRNA. As expected, the formation of the AEP proteolytic product α-Syn N103 corresponded with AEP activity. Moreover, suppression of MPP$^+$-induced AEP activity corresponded with a reduction in MAO-B activity. Interestingly, knockdown of AEP in DMSO controls resulted in increased α-Syn levels, and MAO-B enzymatic activity tightly associated with α-Syn N103 fragmentation, but not total α-Syn levels (Fig 3D–F), indicating that α-Syn N103 might be responsible for promoting MAO-B enzymatic activity. We made similar observations with small molecular AEP inhibitors, compound 11 and MVO (van Kasteren *et al*, 2011; Zhang *et al*, 2017b), which inhibited α-Syn N103 production triggered by MPP$^+$. As expected, AEP enzymatic activity was inhibited by these two compounds. Again, MPP$^+$-stimulated MAO-B activity was significantly suppressed when AEP was inhibited, fitting with the expression pattern of α-Syn N103 (Fig 3G–I).
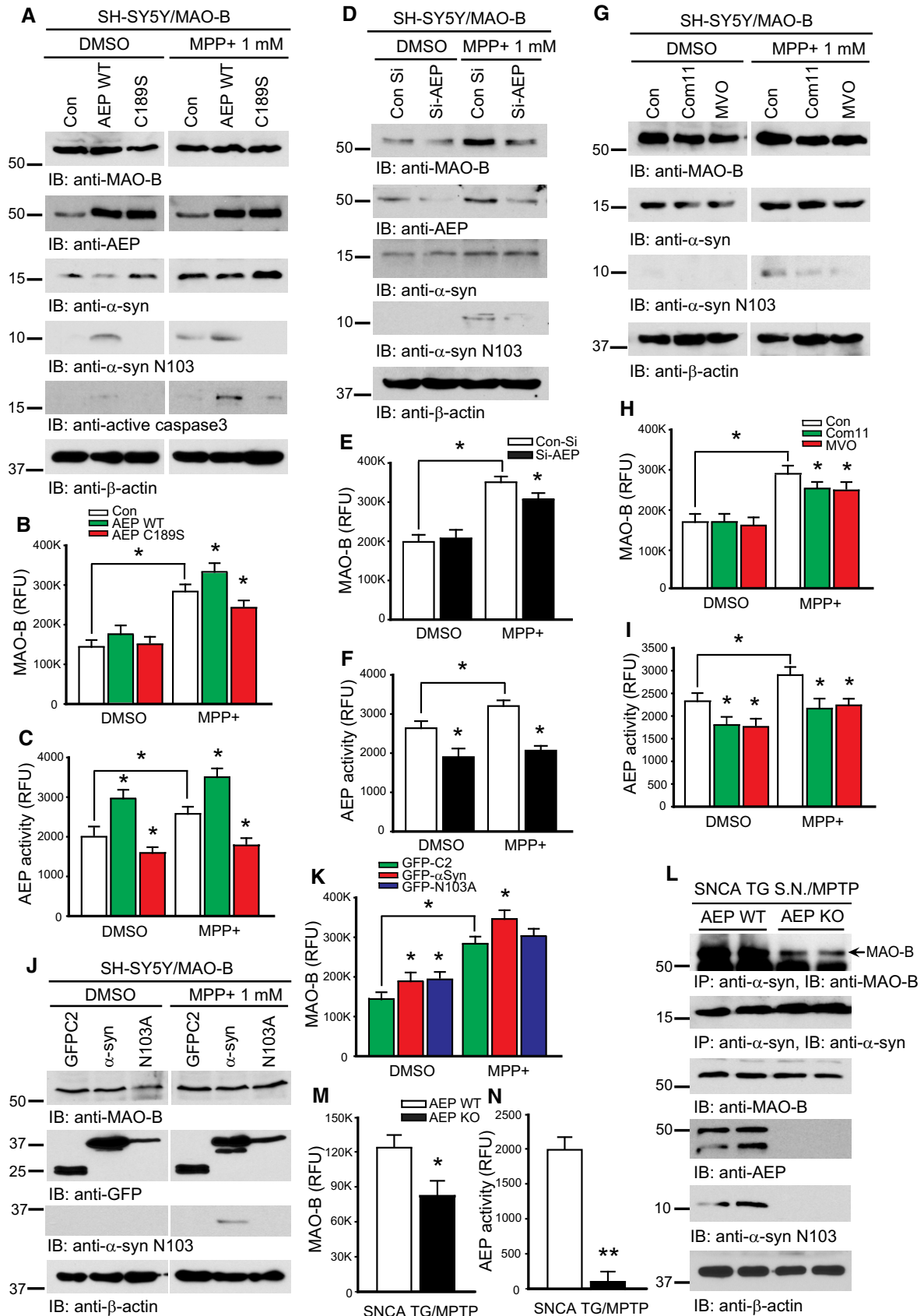
Figure 3.

Figure 3. AEP cleavage of α-Synuclein regulates its stimulatory activity toward MAO-B.

A   AEP increases MAO-B enzymatic activity. AAV-AEP, C189S, and control viruses were added to SH-SY5Y cells, and MAO-B was transfected, followed by MPP$^+$ (1 mM) treatment for 24 h. Immunoblotting was conducted by various antibodies including the specific AEP-cleaved α-Syn N103.

B   MPP$^+$ activates MAO-B via AEP. A MAO-B enzymatic activity assay showed that AEP overexpression increased MAO-B activity after MPP$^+$ treatment. This increase was blocked by AEP C189S.

C   AEP enzymatic activity assay.

D, E   Depletion of AEP diminishes MPP$^+$-induced MAO-B activity. AEP was repressed by siRNA in SH-SY5Y cells and MAO-B was transfected, then followed by MPP$^+$ (1 mM) treatment for 24 h. Immunoblotting was conducted by various antibodies (D). Knockdown of AEP inhibits MPP$^+$-induced MAO-B activity (E).

F   AEP repression by siRNA was verified by an enzymatic activity assay.

G–I   AEP inhibitors block MPP$^+$-induced MAO-B activity. AEP inhibitors, compound 11 (10 μM) and MVO26630 (2 μM), were added in SH-SY5Y cells in 30 min before transfection and MAO-B was transfected, then followed by MPP$^+$ (1 mM) treatment for 24 h. Immunoblotting was conducted by various antibodies (G). Inhibition of AEP decreased MPP$^+$-induced MAO-B activity (H). AEP inhibitory effect was verified by enzymatic activity assay (I).

J, K   α-Syn cleavage by AEP is required for MPP$^+$-induced MAO-B activity. MAO-B was transfected with GFP-C2, GFP- α-Syn, or GFP-N103A in SH-SY5Y cells, followed by MPP$^+$ (1 mM) treatment for 24 h. Immunoblotting verified uncleavable α-Syn N103A by N103 antibody (J). Uncleavable α-Syn N103A abolished MPP$^+$-induced MAO-B activity compared to α-Syn overexpression (K).

L   MPTP induces the association between α-Syn and MAO-B. SNCA TG/AEP WT mice treated with MPTP (30 mg/kg) increase the interaction between α-Syn and MAO-B compared to SNCA TG/AEP KO mice. Immunoprecipitation in substantia nigra tissue of MPTP-treated mice was performed with anti-α-Syn, and the precipitated proteins were analyzed by immunoblotting with anti-MAO-B (top panel). Cell lysates were probed with various antibodies (3rd to bottom panels).

M   MAO-B enzymatic assay shows that AEP knockout in SNCA TG mice inhibits MAO-B activity induced by MPTP *in vivo*.

N   AEP KO mice were confirmed by an AEP enzymatic assay.

Data information: Data are shown as mean ± SEM. $N = 3$ each group. $*P < 0.05$, $**P < 0.01$.

To further investigate the role of AEP cleavage of α-Syn in MAO-B activation, we utilized an uncleavable α-Syn mutant (N103A). Overexpression of wild-type α-Syn and the N103A mutant elevated MAO-B activity under control conditions. However, MPP$^+$-provoked MAO-B activity was abolished in the presence of the N103A mutant as compared with wild-type α-Syn (Fig 3J and K), supporting that N103 cleavage by AEP is indispensable for α-Syn to stimulate MAO-B enzymatic activity. Moreover, MAO-B activity was higher in nigral tissue treated with AAV-α-Syn N103, followed by treatment with AAV-wild-type α-Syn, and AAV-GFP control. AEP enzymatic activity followed the same order (Fig EV3A and B), consistent with the *in vitro* catalytic activity by α-Syn N103 and wild-type α-Syn. Immunoblotting analysis demonstrated that α-Syn N103 overexpression strongly induced nigral MAO-B and AEP expression as compared to α-Syn wild-type or GFP overexpression. In alignment with these observations, TH levels were the lowest following AAV-α-Syn N103 treatment, followed by AAV α-Syn wild-type, and AAV-GFP control treatment (Fig EV3C), suggesting that expression of α-Syn N103 triggers MAO-B activation, leading to AEP upregulation, and subsequent dopaminergic neuronal loss in the SN. To further test the notion that AEP cleavage of α-Syn is crucial for escalating MAO-B activity, we extended our studies into SNCA and SNCA/AEP$^{-/-}$ transgenic mice, treated with MPTP. When AEP was knocked out, α-Syn N103 was absent. Co-immunoprecipitation revealed that α-Syn was strongly associated with MAO-B in SNCA mice, whereas this interaction was reduced in AEP KO mice (Fig 3L). Accordingly, MAO-B and AEP enzymatic activity was significantly reduced in SNCA/AEP$^{-/-}$ mice as compared to SNCA mice (Fig 3M and N). Together, these findings support that AEP-mediated cleavage α-Syn at N103 plays an important role in upregulating MAO-B activities upon MPTP treatment.

MAO-B mediates AEP activation and subsequent α-Synuclein cleavage

3,4-Dihydroxyphenyl acetaldehyde (DOPAL), the catabolic product of MAO-B metabolism of DA, can cause DA neuron death, and is an endogenous neurotoxin which is present in human SN neurons

(Burke, 2003). Thus, we hypothesized that DOPAL may induce AEP activation in dopaminergic cells. To test this possibility, we incubated SH-SY5Y cells with DOPAL for different time points. Subsequent enzymatic assays demonstrated that both AEP and MAO-B were activated by DOPAL in a time-dependent manner (Fig 4B and C). Notably, their protein levels were also raised temporally by DOPAL. In alignment with these findings, α-Syn, especially its AEP cleavage product, α-Syn N103, was upregulated upon DOPAL treatment. α-Syn N103 levels closely followed AEP enzymatic activity (Fig 4A). In addition to upregulation of endogenous AEP, MAO-B, and α-Syn, DOPAL treatment also significantly increased MAO-B activity as compared to control. This activity was further elevated by co-expression of α-Syn constructs (Fig EV4A and B). Noticeably, both DOPAL and MPP$^+$ blocked the enzymatic activity of purified MAO-B recombinant protein in a dose-dependent fashion (Fig EV4C and D), suggesting that these metabolites directly inhibit MAO-B enzymatic activity *in vitro*, but that they activate AEP resulting in cleavage of α-Syn at N103, activating MAO-B. To further explore DOPAL's role in these events, we pretreated SH-SY5Y cells with the MAO-B-specific inhibitor Rasagiline, followed by MPP$^+$ treatment. Rasagiline strongly inhibited MAO-B activity, and MPP$^+$-induced increases in MAO-B activity were also blunted by the inhibitor (Fig 4E). Interestingly, Rasagiline repressed the level of both full-length and cleaved, active, AEP repressing MPP$^+$-triggered AEP activity. MPP$^+$-induced α-Syn N103 cleavage was blocked by Rasagiline as well (Fig 4D–F). Next, in order to further interrogate the role of MAO-B in these effects we transfected SH-SY5Y cells with MAO-A- or MAO-B-specific siRNAs. MPP$^+$-upregulated AEP was reduced, when MAO-B was knocked down. In alignment with these findings, α-Syn N103 cleavage followed the levels of active AEP (Fig 4G). MAO-B siRNA substantially reduced its enzymatic activities with either DMSO or MPP$^+$ treatment (Fig 4H). However, the MPP$^+$-mediated increase in AEP enzymatic activity was inhibited with MAO-B knockdown (Fig 4I). MPTP is converted by MAO-B to MPP$^+$, and MAO-B KO mice are resistant to MPTP (Grimsby *et al*, 1997). To confirm the effect of MAO-B in MPP$^+$-induced AEP activity and neuronal death *in vivo*, we intraperitoneally injected MPTP into the wild-type and MAO-B KO mice. TH immunoreactivity was
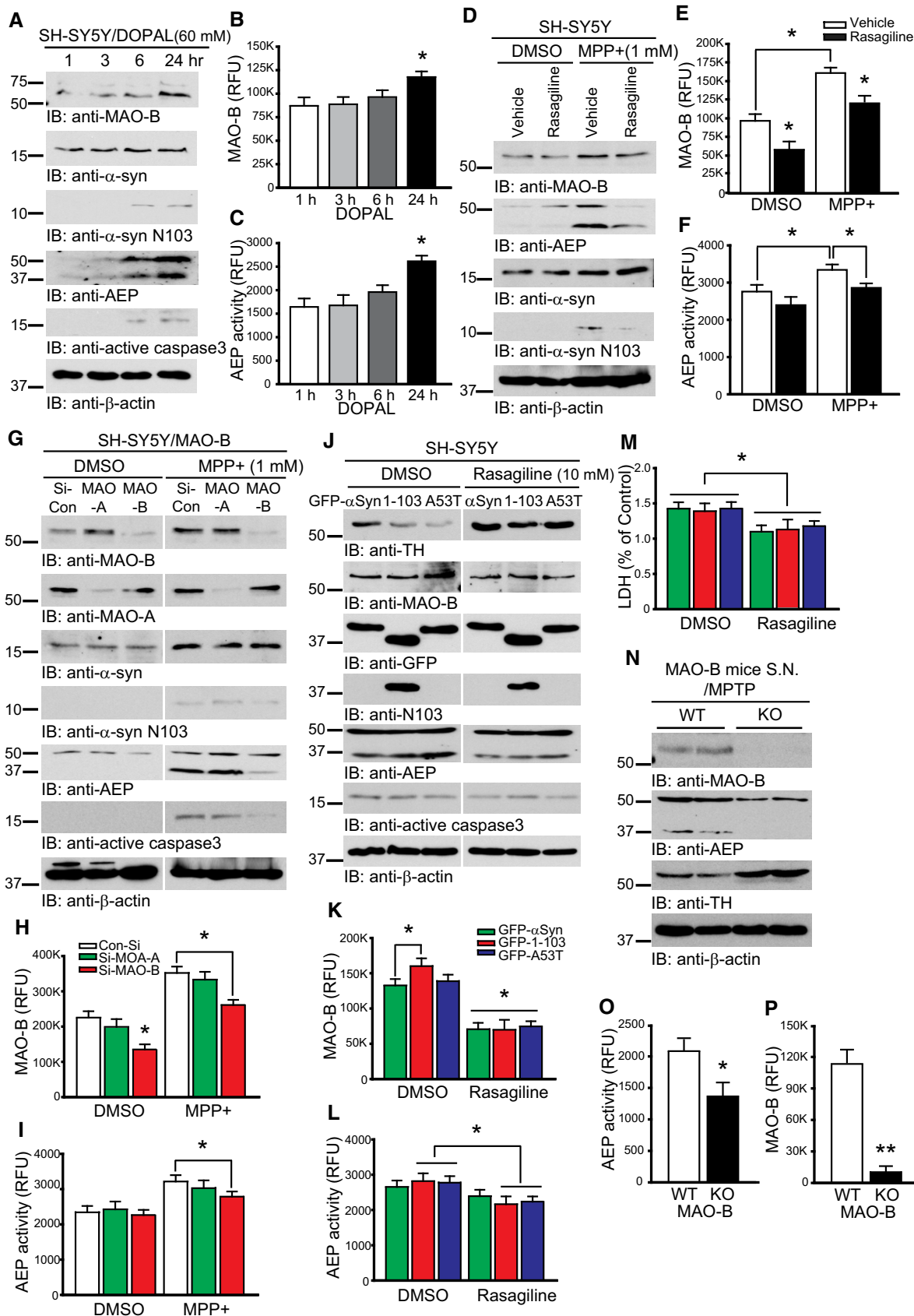
Figure 4.

◀

Figure 4. MAO-B mediates AEP activation and α-Synuclein cleavage.

A   DOPAL increases MAO-B expression in a time-dependent fashion. SH-SY5Y cells were treated with DOPAL (60 μM) for 1, 3, 6, or 24 h, and cell lysates were immunoblotted by various antibodies.

B, C MAO-B and AEP enzymatic assays. DOPAL enhanced MAO-B and AEP activity at 24 h.

D   Inhibition of MAO-B blocks MPP^+-induced AEP activation and α-Syn cleavage. The MAO-B inhibitor, Rasagiline (10 μM), was added to SH-SY5Y cells 30 min before MAO-B transfection, followed by MPP^+ (1 mM) treatment for 24 h. Immunoblotting showed that the Rasagiline inhibited the expression of AEP and N103 after MPP^+ treatment.

E   MAO-B inhibition by Rasagiline was verified by a MAO-B enzymatic activity assay.

F   An enzymatic assay showed that Rasagiline decreased AEP activity.

G   MAO-B and MAO-A were repressed by siRNA in SH-SY5Y cells and MAO-B was transfected, then followed by MPP^+ (1 mM) treatment for 24 h. Immunoblotting was conducted by various antibodies. MAO-B knockdown inhibited the expression of AEP.

H   The repression of MAO-B by siRNA was verified by enzymatic activity assay.

I   Knockdown of MAO-B, but not MAO-A, inhibited MPP^+-induced AEP activity.

J   MAO-B inhibitor prevents dopaminergic cell loss induced by α-Syn. DMSO or Rasagiline was pretreated SH-SY5Y cells 30 min before GFP-α-Syn, GFP-α-Syn 1-103, or GFP-α-Syn A53T were transfected. Immunoblotting showed that Rasagiline rescued TH-positive cell from loss triggered by α-Syn overexpression.

K, L An enzymatic assay showed that Rasagiline inhibited MAO-B and AEP activities in α-Syn-overexpressed cells.

M   LDH assay showed that Rasagiline produced a protective effect against α-Syn-mediated SH-SY5Y cell death.

N   MAO-B KO mice were resistant to MPTP (30 mg/kg) administration-induced TH loss. SN lysates were analyzed by immunoblotting with anti-MAO-B (top panel), AEP, and TH antibodies.

O   AEP enzymatic assay. MAO-B knockout inhibited AEP activity induced by MPTP *in vivo*.

P   MAO-B KO mice were confirmed by MAO-B enzymatic assay.

Data information: Data are shown as mean ± SEM. *N* = 3 each group. *P < 0.05, **P < 0.01.

preserved from the MPTP injury in the SN of MAO-B KO mice as compared with wild-type mice (Fig 4N). MPTP-mediated AEP enzymatic activity was significantly decreased in MAO-B KO mice (Fig 4O). As expected, MAO-B enzymatic activity was diminished in MAO-B KO mice (Fig 4P).

Our data support that the MAO-B-generated DA metabolite, DOPAL, triggers AEP activation and subsequently α-Syn N103 cleavage. α-Syn N103 thereafter binds MAO-B and stimulates its enzymatic activity. To test this, we expressed GFP-tagged α-Syn, α-Syn N103, and A53T in SH-SY5Y cells, followed by treatment with DMSO or Rasagiline. Compared with wild-type α-Syn, overexpression of α-Syn N103 or A53T greatly reduced TH levels, which were rescued by Rasagiline treatment. A MAO-B activity assay showed that α-Syn N103 significantly elevated the enzymatic activity as compared to GFP-α-Syn. As expected, Rasagiline blocked MAO-B activity, no matter which constructs were expressed (Fig 4J and K). Again, α-Syn N103 or A53T-provoked AEP activity was repressed by Rasagiline; accordingly, LDH activity was substantially reduced when MAO-B was blocked, fitting with the neuroprotective feature of Rasagiline (Fig 4L and M). Thus, MAO-B plays a critical role in activating AEP which subsequently cleaves α-Syn at N103, resulting in further activation of MAO-B via a positive feed-back loop.

AEP cleavage of α-Synuclein mediates PD pathologies and motor functions

If α-Syn N103 indeed enhances MAO-B activity, triggering AEP activation via DOPAL and subsequently dopaminergic neurodegeneration, overexpression of AEP in SNCA transgenic mice should facilitate the early onset of PD pathogenesis. To test this possibility, we utilized 3- to 4-month-old wild-type, SNCA KO, and SNCA transgenic mice which do not display any PD pathology or motor dysfunctions. Two months following viral delivery of AAV-AEP or AAV-C189S mutant into the SN, mice were evaluated for motor dysfunction. The rotarod assay showed that overexpression of wild-type AEP but not C189S or GFP control in SNCA transgenic mice resulted in significant motor impairment. No motor impairment was seen in

wild-type or SNCA KO mice (Fig 5A). We made similar observations with wild-type AEP overexpression in both the cylinder test and with amphetamine-induced rotations (Fig 5B and C). The amphetamine-activated effects in mice behavior are induced primarily by dopamine release in the terminal regions of dopaminergic system, especially striatum. Due to ipsilateral damage of striatum by AEP overexpression in SNCA TG mice, only this group showed one side preferred rotation, when amphetamine was injected intraperitoneally (Fig 5C). Densitometric immunofluorescent staining of TH on both the striatum and the SN showed that wild-type AEP overexpression induced TH loss in both regions, whereas it failed to produce dopaminergic cell loss in wild-type or SNCA KO mice, corresponding with the motor impairment (Fig 5D–F). Immunoblotting confirmed that AEP was highly expressed in the SN of these animals (Fig 5G, 5th panel). A co-immunoprecipitation assay showed that α-Syn exhibited a stronger association with MAO-B in SNCA transgenic mice as compared to wild-type mice. Moreover, α-Syn N103 was highly elevated in SNCA transgenic mice treated with AAV-AEP, correlating with the high degree of MAO-B co-precipitation in these samples. By contrast, in SNCA KO mice there was no MAO-B co-precipitation, no matter whether wild-type AEP or C189S was overexpressed (Fig 5G). As expected, AEP activity was much higher in mice treated with wild-type AEP as compared to C189S or control (Fig 5H). MAO-B activity was markedly elevated with wild-type AEP overexpression in SNCA transgenic mice but not in other mice (Fig 5I), which is consistent with the observation of dopaminergic neurodegeneration loss and motor deficits. HPLC analysis of DOPAC, a metabolite of DA from MAO-B, further confirmed that MAO-B was selectively activated by wild-type AEP in α-Syn transgenic mice (Fig 5J), fitting with the increase in α-Syn N103 in these mice.

Asparagine endopeptidase is an age-dependent protease that cleaves α-Syn in PD brains (Zhang *et al*, 2017a). Wild-type SNCA transgenic mice display PD-like pathology and motor deficits between 12 and 18 months of age (Janezic *et al*, 2013). To determine whether AEP cleavage of α-Syn in SNCA transgenic mice induces MAO-B activation in an age-dependent manner, we analyzed 3, 7, and 12 months old wild-type, KO, and SNCA
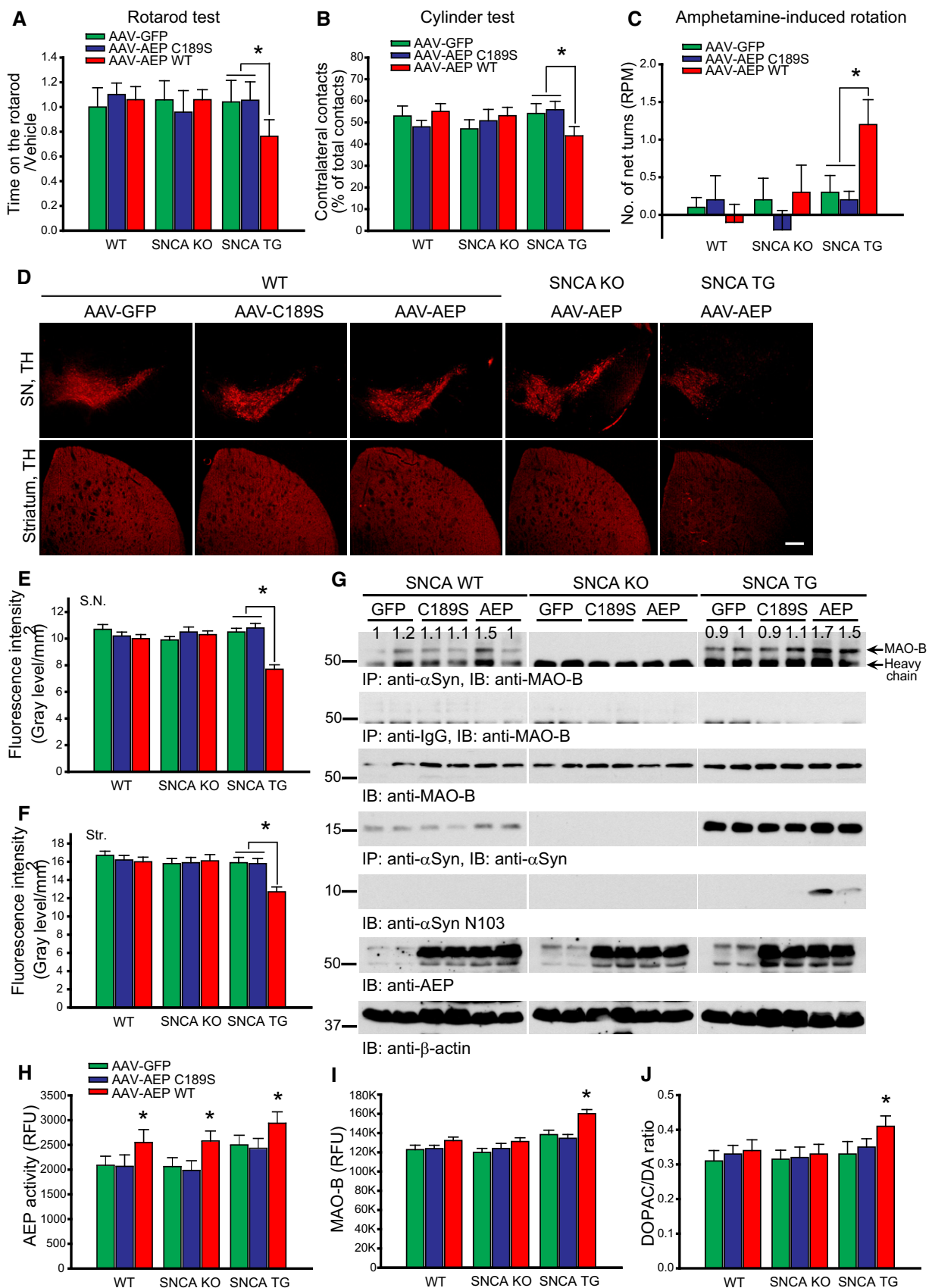
Figure 5.

◀

Figure 5. AEP cleavage of α-Synuclein mediates PD pathologies and motor defects.

A–C   AEP overexpression induces motor dysfunction in SNCA mice. AAV-GFP, AAV-AEP, or AAV-AEP C189S were injected into right substantial nigra of SNCA WT, KO, or TG mice. Motor behavioral assays, rotarod (A), cylinder test (B), and amphetamine-induced rotation (C), were conducted by a blinded observer 2 months after the virus injection. AAV-AEP infection induces motor dysfunction in SNCA TG mice. N = 7–9 each group.

D   TH expression in substantial nigra (SN) and striatum of the above animals was analyzed by immunofluorescent staining. Scale bar is 200 μm.

E, F   Quantification of TH-positive fluorescent signals in SN (E) and striatum (F). N = 3 each group.

G   AEP enhances the interaction between MAO-B and α-Syn in SNCA TG mice. Co-immunoprecipitation assay with anti-α-Syn from SN tissues and co-precipitated proteins were analyzed by immunoblotting. Densitometric quantification normalized by each α-Syn immunoblot was marked in the image. SN lysates were probed by various indicated antibodies.

H   AEP enzymatic assay. AEP activity was increased in the SN of AAV-AEP WT-injected mice but not in the dominant-negative mutant, AEP C189S-injected groups. N = 3 each group.

I   MAO-B activity was increased in the AEP WT-injected group of SNCA TG mice. N = 3 each group.

J   The ratio of DOPAC/DA in SN was increased by the infection of AAV-AEP in SNCA TG mice. N = 3 each group.

Data information: Data are shown as mean ± SEM. N = 3 each group. *$P < 0.05$.

transgenic mice and compared AEP and α-Syn N103 expression levels in these mice. We found that AEP was indeed upregulated in an age-dependent manner in all of the mice. However, its concentrations were the highest in SNCA transgenic mice, as were the levels of mature and active 36-kD AEP. Accordingly, α-Syn N103 specifically appeared in 12-month-old SNCA transgenic mice but not in younger mice of any genotype, corresponding with the AEP activation pattern. Notably, α-Syn expression levels were also escalated in an age-dependent manner and the interaction with MAO-B was increased in the corresponding temporal pattern, with the highest degree of interaction seen in 12-month-old SNCA mice (Fig EV5A). Accordingly, MAO-B activity was the highest in 12-month-old SNCA mice, which was validated by quantitative analysis of DOPAC/DA ratios in these mice (Fig EV5B and C). Thus, AEP cleaves α-Syn at N103 in an age-dependent manner which results in the subsequent increase in MAO-B activity.

Inhibition of MAO-B abolishes α-Synuclein-induced PD pathologies

To explore the role of the association of α-Syn with MAO-B in PD pathogenesis, we injected AAV virus expressing α-Syn into the SN of wild-type mice (3 months old), followed by Rasagiline treatment in the drinking water for 15 weeks. Compared to GFP control, overexpression of α-Syn resulted in marked nigral TH neuron loss and nigrostriatal denervation, which was significantly reduced by Rasagiline (Fig 6A and D–F). The cylinder test and rotational asymmetry showed an impairment congruent with the loss of dopaminergic neurons, and these motor deficits were reduced with Rasagiline treatment (Fig 6B and C). An MAO-B enzymatic activity assay and quantitative DOPAC/DA analysis in both SN and striatum tissues showed that overexpression of α-Syn greatly increased MAO-B activity, resulting in an increase in the DOPAC/DA ratio, which was strongly inhibited by Rasagiline (Fig 6G and H). AEP enzymatic activity corresponded to the MAO-B activity (Fig 6I and J), indicating that these two enzymes might be tightly coupled with each other in PD pathogenesis. Immunoblotting of nigral tissue confirmed that α-Syn overexpression resulted in an increase in mature and active AEP levels and the subsequent increase in α-Syn N103 cleavage, which were repressed by Rasagiline treatment. As expected, TH levels as measured by immunoblotting were reduced by α-Syn overexpression, and this reduction was rescued by MAO-B inhibition (Fig 6K). Therefore, these data support that inhibition of MAO-B

diminishes AEP activity and thus reduces α-Syn overexpression-mediated PD pathology and motor dysfunction.

α-Synuclein N103 fragment fails to induce PD pathogenesis in MAO-B KO mice

We recently reported that α-Syn N103 promotes α-Syn aggregation triggering dopaminergic neurodegeneration, leading to PD pathogenesis (Zhang *et al*, 2017a). Moreover, inhibition of MAO-B suppressed α-Syn-mediated PD pathology, which was associated with reduced α-Syn N103 cleavage by AEP. To directly interrogate the role of α-Syn N103 in binding and activating MAO-B in PD pathogenesis, we injected AAV expressing α-Syn N103 into the SN of wild-type and MAO-B-null mice (3 months old). Two months after the vector delivery, a densitometric analysis of TH immunofluorescence of both the SN and the striatum demonstrated that α-Syn N103 overexpression resulted in significantly reduced neurotoxicity in MAO-B-null mice as compared with wild-type mice (Fig 7A and E–G). In alignment with our findings above, MAO-B-null mice injected with α-Syn N103 virus were partially spared from motor deficits as compared with wild-type mice (Fig 7B–D). Together, these data indicate that MAO-B activity is required for α-Syn N103-mediated toxicity. Immunoblotting verified that α-Syn N103 expression in both wild-type and MAO-B-null mice. Corresponding to the histological findings, TH immunoreactivity was significantly reduced in α-Syn N103-expressing brains as compared with those expressing GFP control in wild-type mice, and it remained comparable in MAO-B KO mice (Fig 7H). α-Syn N103 overexpression produced greatly decreased striatal dopamine concentrations in wild-type mice as compared to AAV-GFP-treated controls. However, dopamine levels were significantly higher in MAO-B-null mice as compared with wild-type mice (Fig 7I). As expected, MAO-B activity was highly elevated by α-Syn N103 expression in wild-type mice, but was not detected in MAO-B-null mice (Fig 7J). Asparagine endopeptidase was highly activated by α-Syn N103 in wild-type mice, and this activity was markedly reduced in MAO-B-null mice regardless of GFP or α-Syn N103 overexpression (Fig 7K), in accordance with active AEP in immunoblotting analysis (Fig 7H, 3rd panel). Taken together, these data strongly suggest that α-Syn N103 binds and stimulates MAO-B enzymatic activity that is required for its deleterious pathological activities, supporting that AEP cleavage of α-Syn is essential for its etiopathological effect in PD.
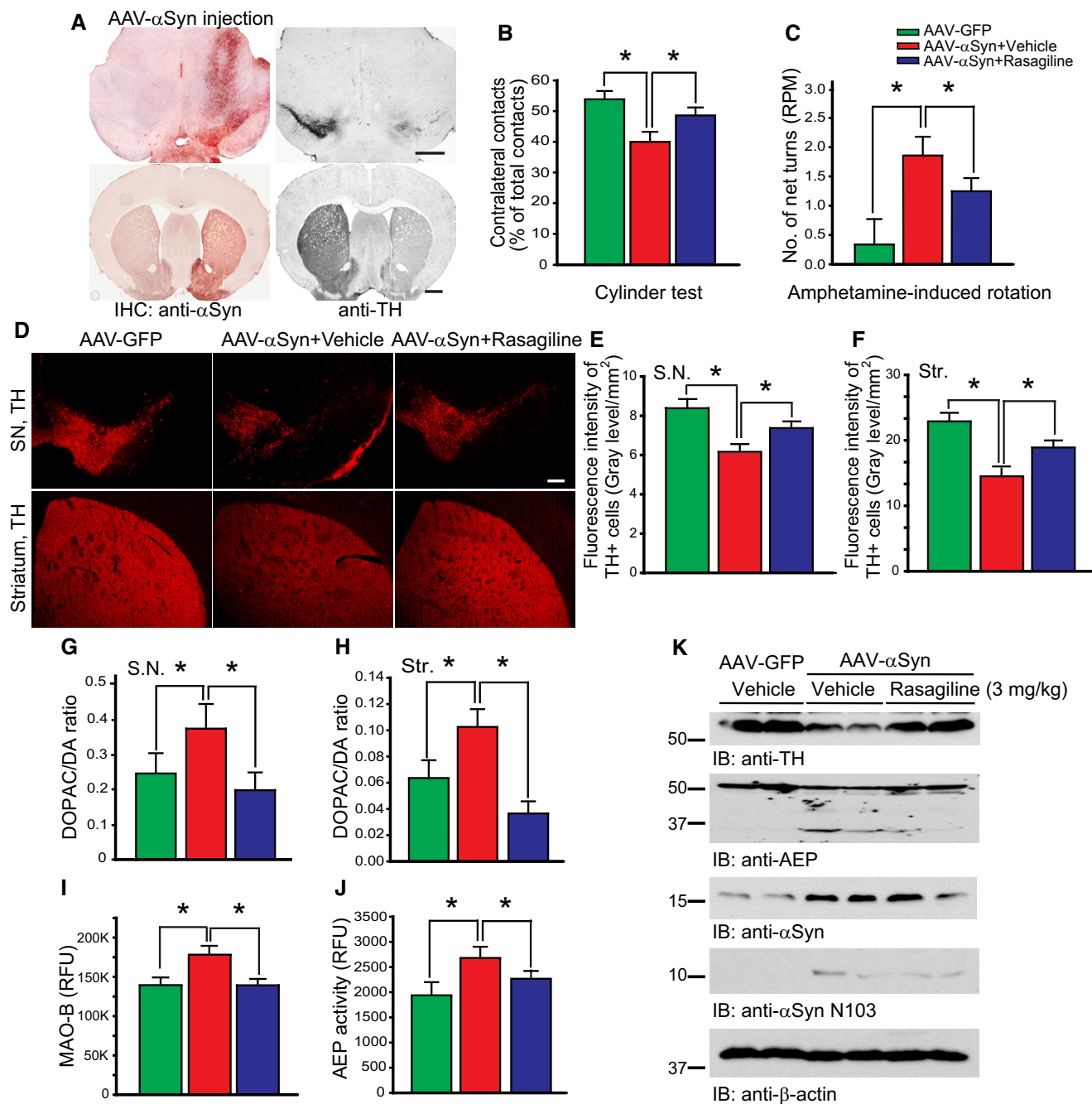
Figure 6. Inhibition of MAO-B abolishes α-Synuclein-induced PD pathologies.

A   α-Syn induces TH loss in SN. C57BL/6 mice were injected with AAV-GFP or AAV-α-Syn into right substantial nigra, and drinking water including Rasagiline (3 mg/kg/day) or vehicle was administered for 15 weeks. AAV-α-Syn injection into SN was confirmed by immunohistochemistry using an α-Syn antibody. TH-staining showed TH+ dopaminergic cell loss in SN and striatum ipsilateral to the AAV-α-Syn injection. Scale bar is 500 μm.

B, C   MAO-B inhibitor blocks α-Syn-induced motor impairment. The motor defects of α-Syn-injected animals were analyzed by motor functional assays, cylinder test (B), and amphetamine-induced rotation (C). Rasagiline significantly improved the α-Syn-induced motor impairment. N = 9 each group..

D   Rasagiline reduces TH loss induced by α-Syn. TH expression in substantial nigra (SN) and striatum of the above animals was analyzed by immunofluorescent staining. Scale bar is 200 μm.

E, F   Quantification of TH-positive fluorescent signaling in SN (E) and striatum (F). N = 3 each group.

G, H   The increase in DOPAC/DA ratio by α-Syn was blocked by Rasagiline in α-Syn-injected mice. N = 3 each group.

I, J   MAO-B and AEP enzymatic assays. MAO-B (I) and AEP activity (J) were increased in the SN of AAV-α-Syn-injected mice, and Rasagiline inhibited α-Syn-induced enhancement of this activity. N = 3 each group.

K   Rasagiline restores TH expression of α-Syn-injected mice. The reduction in AEP and α-Syn N103 fragment by Rasagiline in SN lysates was analyzed by immunoblotting.

Data information: Data are shown as mean ± SEM. N = 3 each group. *P < 0.05.

Figure 7. α-Synuclein N103 fragment fails to induce PD pathogenesis in MAO-B KO mice.

A   Viral injection into SN. AAV-GFP or AAV-α-Syn N103 was injected into the right substantia nigra of MAO-B WT or KO mice. AAV-α-Syn N103 injection into SN was confirmed by immunohistochemistry using α-Syn N103 antibody. Scale bar is 500 μm.

B–D   Motor behavioral tests. The motor defects of α-Syn N103-injected animals were recovered in MAO-B KO mice. Various behavior assays including rotarod (B), cylinder test (C), and amphetamine-induced rotation (D) showed that MAO-B KO mice were resistant to AAV-α-Syn N103-induced toxicity. N = 8 each group.

E   MAO-B KO reduces TH loss induced by α-Syn N103. TH expression in substantia nigra (SN) and striatum of the above animals was analyzed by immunofluorescent staining. Scale bar is 200 μm.

F, G   Quantification of TH-positive fluorescent signals in SN (F) and striatum (G). N = 3 each group.

H   SN lysates from each group were analyzed by immunoblotting. The reduction in TH expression by α-Syn N103 infection was restored in MAO-B KO mice compared to WT.

I   The increase in DOPAC/DA ratio by α-Syn N103 was blocked in MAO-B KO mice. N = 3 each group.

J   MAO-B KO mice were confirmed by MAO-B enzymatic assay. MAO-B activity was increased by α-Syn N103 in WT mice. N = 3 each group.

K   AEP activity was increased in AAV-α-Syn N103-injected group of WT mice, and it was reduced in MAO-B KO mice compared to α-Syn N103-injected WT mice. N = 3 each group.

L   A schematic model for AEP-cleaved α-Syn N103 triggering MAO-B activation that feeds forward to further activate AEP by DA metabolite DOPAL.

Data information: Data are shown as mean ± SEM. N = 3 each group. *P < 0.05.

Discussion

In this report, we have identified the direct association between α-Syn and MAO-B, two major pathological players in PD. Interestingly, the C-terminal-truncated α-Syn N103 fragment displays the strongest binding activity toward MAO-B, co-localizing in the mitochondria. Compared to full-length α-Syn, the α-Syn N103 truncate is more efficient in stimulating MAO-B enzymatic activity. We recently showed that AEP is highly activated in PD patient brains and cleaves α-Syn at N103 residue in an age-dependent manner. Importantly, N103 cleavage greatly escalates α-Syn aggregation and neurotoxicity (Zhang *et al*, 2017a). In the current study, we demonstrate that AEP cleavage of α-Syn N103 is required for MPTP-induced MAO-B activation. Overexpression of AEP wild-type, but not the dominant-negative C189S mutant, in young SNCA transgenic mice induces α-Syn N103 cleavage and the subsequent binding to, and activation of, MAO-B. Activation of MAO-B facilitates the early onset of PD pathogenesis and the appearance of motor impairments (Fig 5). Asparagine endopeptidase is highly expressed in SNCA transgenic mice and α-Syn N103 cleavage, and the subsequent MAO-B activation occurs in an age-dependent way and is only apparent in 12-month-old mice (Fig EV5). On the other hand, we also show that the MAO-B DA metabolite, DOPAL, activates AEP in SH-SY5Y cells and induces α-Syn N103 cleavage that subsequently enhances MAO-B activity on its own. Accordingly, blockade of MAO-B with its inhibitor Rasagiline or silencing of MAO-B with siRNA inhibits MPP^+-triggered AEP activation or α-Syn N103 production (Fig 4). Consequently, Rasagiline inhibits α-Syn overexpression-induced PD pathology and motor deficits (Fig 6). Furthermore, knockout of MAO-B completely abolishes α-Syn N103-induced neurotoxicity (Fig 7). Hence, our findings strongly support the model that MAO-B is necessary for α-Syn N103-mediated PD neurotoxicity (Fig 7L). In this model, and consistent with our findings, inhibition of AEP prevents α-Syn N103 production and suppresses MAO-B activation, providing a disease-modifying therapeutic interference strategy for PD.

Rasagiline, an irreversible inhibitor of MAO-B, is a propargylamine, a family of molecules considered to have neuroprotective potential in PD (Schapira & Olanow, 2008). Rasagiline provides protection against a number of *in vitro* dopaminergic toxins including 6-hydroxydopamine (6-OHDA), MPP^+, β-amyloid, tetrahydroisoquinoline, and serum and growth factor deprivation, and is protective in animal models (Mandel *et al*, 2005; Schapira, 2008). Surprisingly, this protection is not dependent upon the MAO-B inhibitory action, because the inactive S-enantiomer of Rasagiline is as potent as the active form in protection studies, and the protective action is seen in cells that do not express MAO-B (Youdim & Weinstock, 2001; Youdim *et al*, 2001; Maruyama *et al*, 2003). It has been proposed that Rasagiline exerts its protection through an anti-apoptotic effect that may be mediated by activation of Bcl-2 and Bcl-xL and the protein kinase C-/mitogen-activated protein kinase (PKC/MAPK) pathway, and down-regulation of pro-apoptotic molecules such as Bax and Bad (Mandel *et al*, 2005; Youdim *et al*, 2005). Moreover, it has been reported that Rasagiline induces an increase in cellular glutathione levels, a reduction in superoxide generation, and a trend to ameliorate the fall in mitochondrial membrane potential, supporting a role for Rasagiline in protecting dopaminergic cells against free radical-mediated damage and apoptosis in the presence of α-Syn overexpression (Chau *et al*, 2010). Here, we demonstrate that Rasagiline protects against cell death induced by α-Syn wild-type, α-Syn N103, or A53T mutant overexpression as well as from MPP^+ treatment, and this protection might be associated with a reduction in both MAO-B and AEP enzymatic activities and a reduction in caspase-3 activation (Figs 2–4).

The high selectivity of dopaminergic neuronal degeneration in PD supports the hypothesis that catecholamine neurons produce specific neurotoxins whose accumulation might trigger neuronal death. The idea that MAO-B plays a central role in neuropathogenesis of PD is supported by data showing that aldehydes such as DOPAL generated from catecholamine oxidation by MAO-B might promote oxidative stress and neuronal death. Therefore, the "catecholaldehyde hypothesis" posits a causal link between these two central pathologic players: α-Syn and MAO-B, which is mediated by DOPAL, the most toxic dopamine metabolite. DOPAL is capable of reacting with proteins via the formation of Schiff base and displays a degree of toxicity *in vivo* and *in vitro* that is 100- to 1,000-fold greater than that observed for DA (Anderson *et al*, 2011). The generation of ROS, notably superoxide, during the oxidation of DOPAL to its quinone derivative might, in part, explain the high toxicity of DOPAL and its connection with PD. Several studies have suggested that oxidative stress causes accumulation α-Syn protofibrils (Conway *et al*, 2001) and promotes oligomerization (Norris *et al*, 2003). The
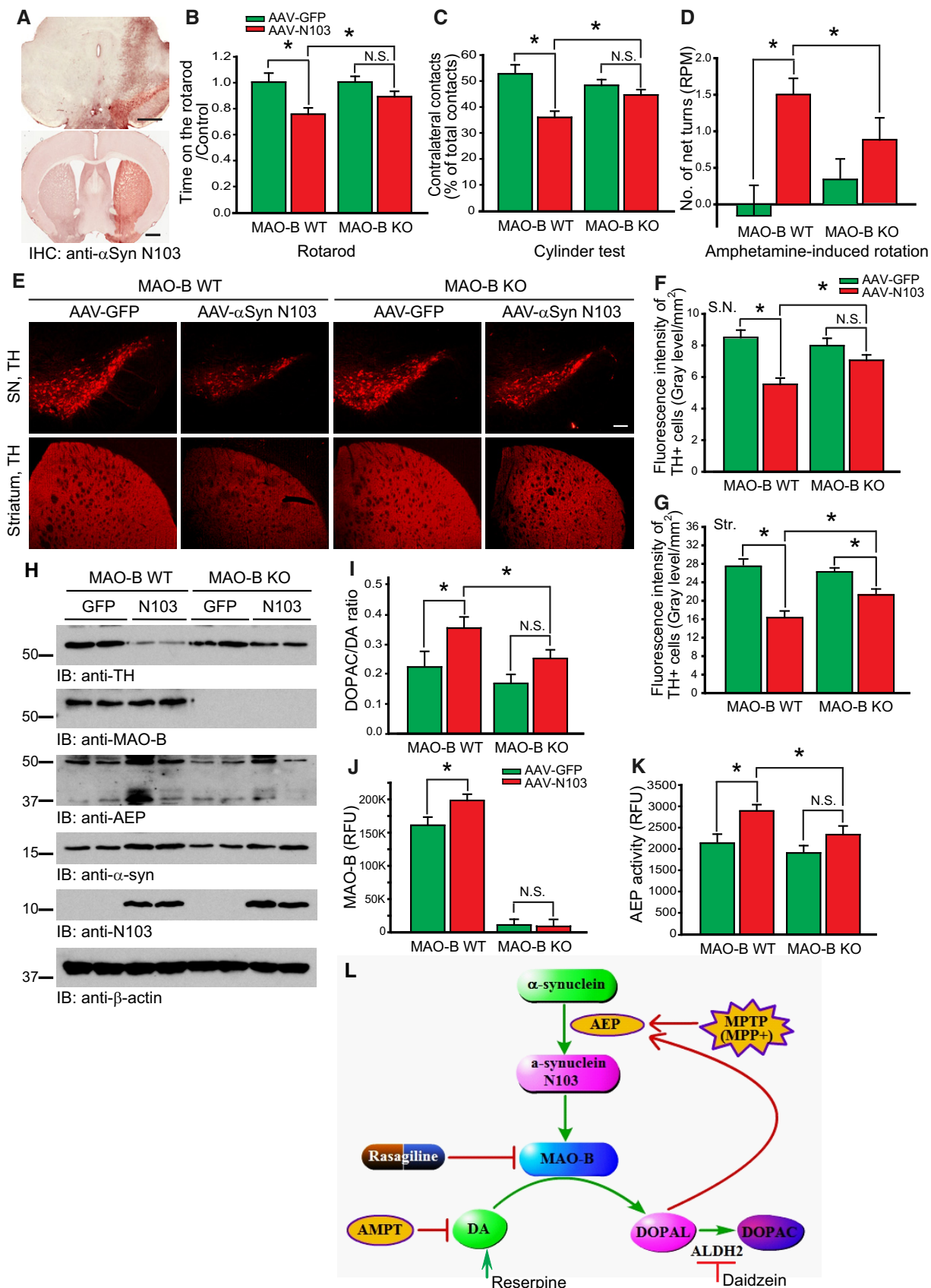
Figure 7.

interaction of α-Syn with either oxidized derivatives of dopamine (e.g., dopaminochrome) or DOPAL could lead to an increase in the rate of formation potentially toxic protein aggregates. Extensive experimental evidence for DOPAL's toxicity and potential involvement in PD has been summarized in recent work and points to its role in covalently crosslinking the highly abundant α-Syn as a possible etiological culprit (Burke *et al*, 2008; Panneton *et al*, 2010; Goldstein *et al*, 2014). One reason why dopaminergic neurons of the VTA are spared from these effects may be because many genes involved in synaptic plasticity and cell survival (neuroprotection, detoxification) are expressed much more abundant in VTA than SN as revealed by microarray analyses (Grimm *et al*, 2004). Moreover, Galter *et al* (2003) confirmed the significant reduction in ALDH expression in SN, but not VTA of PD patients, even though ALDH is highly expressed in both SN and VTA of controls. The different detoxification ability of DOPAL by ALDH might be the one reason to explain the different vulnerabilities, because DOPAL is the main molecule in our mechanism via α-Synuclein/MAO-B/DOPAL/AEP/α-Synuclein N103.

We recently reported that AEP is prone to be activated in the SN as compared to the cortex and cleaves α-Syn at N103 in an age-dependent manner (Zhang *et al*, 2017a). Conceivably, AEP in dopaminergic neurons is more readily activated by the oxidative catecholamine aldehyde. Accordingly, we have demonstrated that DOPAL triggers AEP activation in SH-SY5Y cells inducing α-Syn N103 production and the subsequent increase in MAO-B activity (Fig 4). The "catecholaldehyde hypothesis" suggests that an endogenous neurotoxin unique to dopamine-producing cells causes or contributes to their death in PD (Panneton *et al*, 2010; Goldstein *et al*, 2014). Following biosynthesis or synaptic transmission and reuptake of dopamine, it is either sequestered into storage vesicles or catabolized to prevent its accumulation in the cytosol. The first and obligate step in dopamine metabolism is conversion of the amine group to an aldehyde, producing DOPAL, by MAO-B. The aldehyde is then enzymatically oxidized to a carboxylic acid or reduced to a hydroxyl (Burke *et al*, 2003, 2004). On the other hand, MAO-B oxidizes the xenobiotic MPTP into MPP^+, which is the active neurotoxic compound that is selectively taken up into dopaminergic neurons (Javitch *et al*, 1985), and triggers acute release and chronic depletion of dopamine. Presumably, MPP^+ kills dopaminergic neurons by inhibiting energy metabolism in the mitochondrion (Ramsay & Singer, 1986). Further, MPP^+ inhibition of mitochondrial complex I that synthesizes NAD (nicotinamide adenine dinucleotide), a cofactor for ALDH, results in an elevation of DOPAL concentration and death of DA neurons (Lamensdorf *et al*, 2000; Burke *et al*, 2003). As expected, depletion of dopamine with AMPT (alpha-methyl-p-tyrosine), a tyrosine hydroxylase inhibitor, decreased MPP^+-mediated AEP activation and α-Syn N103 generation, leading to a reduction in the α-Syn N103/MAO-B association and a decrease in the enzymatic activity of MAO-B. Consequently, AMPT rescued MPP^+-triggered dopaminergic cell loss (Fig EV6A–C). Conversely, an increase in DOPAL by treatment with the ALDH inhibitor Daidzein, or Reserpine, a VMAT inhibitor, enhanced both α-Syn N103 cleavage and MAO-B levels, resulting in their increased interaction. The maximal effect was seen with the combination of Reserpine and Daidzein. The subsequent activation of AEP leads

to a loss of TH neurons (Fig EV6D). Moreover, MAO-B and AEP enzymatic activity is tightly coupled with their expression levels (Fig EV6E–F). Accordingly, inhibition of MAO-B attenuates MPTP neurotoxicity (Chen *et al*, 2002) and MAO-B KO mice are resistant to MPTP (Grimsby *et al*, 1997). In the current work, we show that neurotoxic α-Syn N103 was unable to induce PD pathogenesis in MAO-B-null mice (Fig 7). Thus, these findings support that MAO-B plays a central role in α-Syn- or MPTP-induced neurodegeneration.

MPTP induces C/EBPβ, which is a transcription factor related to inflammatory response. C/EBPβ increases α-Syn protein expression and is a potential transcription factor that is susceptible to the promoter regionFig of the α-Syn (Gomez-Santos *et al*, 2005). Noticeably, both α-Syn and MAO-B are upregulated in PD patients (Fig 1), fitting with previous reports (Riederer & Jellinger, 1983; Saura *et al*, 1994; Mahy *et al*, 2000). We have recently reported that α-Syn N103 is escalated in PD brains (Zhang *et al*, 2017a). Previous studies show that truncation of the C-terminal-disordered highly acidic and proline-rich region enhances α-Syn aggregation (Murray *et al*, 2003; Li *et al*, 2005; Wakamatsu *et al*, 2008). Consistent with these findings, our mapping assay demonstrates that 1–103 fragment possesses the strongest binding activity, whereas the truncate of a.a. 1–65 or a.a. 65–140 weakly associates with MAO-B. Human MAO-B crystallizes as a dimer with a hydrophobic bipartite elongated cavity. Depending on the substrate or bound inhibitor, it can exist in either an open or a closed form, which has been shown to be important in defining the inhibitor specificity of MAO-B (Edmondson *et al*, 2007). We observed that α-Syn N103 binds MAO-B on the outer membrane of the mitochondrion and enhances its enzymatic activity (Fig EV1). Presumably, some residues in α-Syn N103, which is involved in protein fibrillogenesis, directly binds MAO-B and modulates its enzymatic activity. Taken together, our data strongly support the model that α-Syn directly associates with MAO-B and catalyzes its enzymatic activity, leading to upregulation of the neurotoxic catecholamine aldehyde metabolite DOPAL from DA, which triggers AEP activation. The elevated AEP subsequently cleaves α-Syn N103, a form of α-syn that displays stronger binding affinity and catalytic activity toward MAO-B; ultimately, this feed-forward loop of increasing activation results in dopaminergic neurodegeneration (Fig 7L). Our findings serve as the foundation for a new mechanistic model explaining how α-Syn and MAO-B interact in PD pathogenesis; in this model, AEP plays a crucial role to amplify the deleterious effect by promoting both α-Syn proteolytic cleavage and further activation of MAO-B.

Materials and Methods

Animals

All mice were obtained from the Jackson Laboratory. Eight- to 12-week-old C57BL/6 were used as controls. SNCA-null mice (B6;129X1-*Snca^{tm1Rosl}*, stock NO. 003692), human SNCA overexpressing mice (B6.Cg-Tg(SNCA)OVX37Rwm *Snca^{tm1Rosl}*/J, stock NO. 023837), or MAO-B knockout mice (B6;129S-Maob^{tm1Shin}/J, stock NO. 014133) on pure genetic background were backcrossed.

The AEP-knockout mice on a mixed 129/Ola and C57BL/6 background were generated as previously reported (Liu *et al*, 2008). Animal care and handling was performed according to the Declaration of Helsinki and Emory Medical School guidelines. Investigators were blinded to the group allocation during the animal experiments. The protocol was reviewed and approved by the Emory Institutional Animal Care and Use Committee.

Human tissue samples

Post-mortem brain frozen samples of PD patients ($N = 3$) and paraffin-embedded sections of PD patients ($N = 3$) were provided from the Emory Alzheimer's Disease Research Center. The study was approved by the biospecimen committee in Emory University. LBD and PD cases were clinically diagnosed and neuropathologically confirmed. Informed consent was obtained from all cases.

Plasmid clones and viral genomes

AAV viral genome contained either the human α-Syn, AEP, or the GFP coding sequence controlled by the hybrid chicken beta-actin/cytomegalovirus promoter. AAV2/5 and LV pseudotyped with VSV-G were produced as described previously (Benskey *et al*, 2016).

Transfection and viral infection of the cells

HEK293 cells and SH-SY5Y cells were transfected with plasmids encoding mGST, Myc, or GFP-tagged α-Synuclein, point mutant α-Synuclein, MAO-B, or MAO-A using polyethylenimine (PEI) or Lipofectamine 3000 (Thermo Fisher Scientific). AAV-AEP, AAV-AEP C189S, AAV-GFP, Lenti-ShRNA-α-Syn, or Lv-α-Syn were used for infection in SH-SY5Y cells. The neurotoxicity was analyzed using LDH assay (CytoTox 96® Non-Radio, Promega).

Western blot analysis

The cultured cells, mouse brain, or human tissues were lysed in lysis buffer (50 mM Tris, pH 7.4, 40 mM NaCl, 1 mM EDTA, 0.5% Triton X-100, 1.5 mM Na_3VO_4, 50 mM NaF, 10 mM sodium pyrophosphate, 10 mM sodium β-glycerophosphate, supplemented with a cocktail of protease inhibitors), and centrifuged for 15 min at 16,000 *g*. The supernatant was boiled in SDS loading buffer. After SDS–PAGE, the samples were transferred to a nitrocellulose membrane. Primary antibodies to the following targets were used: GST-HRP, alpha-tubulin, beta-actin (Sigma-Aldrich), myc, GFP, anti-α-Synuclein, S129 (Santa Cruz), N103, MAO-B (GeneTex), MAO-A (Sigma-Aldrich), anti-TH (Sigma-Aldrich), anti-AEP (6E3, gifted from Dr. Colin Watts's lab), anti-aggregated α-Synuclein (Millipore), MFN1 (Santa Cruz).

Immunostaining

Paraffin-embedded human brain sections or free-floating mouse brain sections sliced by cryotome were treated with 0.3% H_2O_2 for 10 min. Sections were washed three times in PBS and blocked in 1% BSA, 0.3% Triton X-100, for 30 min, followed by overnight incubation with TH antibody (1: 1,000), anti-α-Synuclein, or N103

antibody (1: 500) at 4°C. The signal was developed using Histostain-SP kit (Invitrogen). For immunofluorescence, the sections were incubated overnight with various primary antibodies, TH, MAO-B, N103, or TOMM20 (1: 500), at 4°C. Then, the sections were incubated with the matched fluoro-conjugated secondary antibody for 2 h at room temperature, after three times washing in PBS. The slides were washed three times in PBS and covered with a glass using mounting solution, after DAPI staining for 5 min.

Immunoprecipitation

The mouse brain tissue samples or cultured cells were lysed in lysis buffer and centrifuged for 15 min at 16,000 *g*. The supernatant was incubated with anti-α-Synuclein or GFP antibody and protein A/G-agarose overnight at 4°C. After extensive washing, the bound proteins were eluted from the beads by boiling in sample buffer and subjected to Western blot analyses.

AEP activity assay

Assay buffer (20 mM citric acid, 60 mM Na_2HPO_4, 1 mM EDTA, 0.1% CHAPS and 1 mM DTT, pH 6.0) of 100 μl including 100 μM AEP substrate Z-Ala-Ala-Asn-AMC (ABchem) was added to cell or tissue lysates. AMC released by substrate cleavage was quantified using a fluorescence plate reader at 460 nm for 1 h in kinetic mode.

MAO-B activity assay

Cell or tissue lysates (20 μg) were incubated with the working solution of 100 μl containing 400 μM Amplex Red reagent, 2 U/ml HRP, and 2 mM benzylamine substrate (Molecular Probes). The fluorescence of MAO-B activity was measured in a fluorescence plate reader using excitation in the range of 530–560 nm and emission at 590 ± 10 nm at 37°C for 2 h in kinetic mode.

HPLC analysis

Dopamine and DOPAC levels were determined by HPLC with coulometric detection. Brain samples were homogenized in 0.1 N $HClO_4$ solution (containing 0.01% sodium metabisulfite and 25 ng/ml internal standard 3,4-dihydroxybenzylamine HBr) and centrifuged at 13,000 *g* for 15 min at 4°C. Aliquots of supernatant fractions were filtered with a 0.2-μm HT Tuffryn membrane (Pall), then injected into an Ultrasphere 5 μm ODS column, 250 × 4.6-mm (Hichrom Limited) and separated with a mobile phase containing 0.1 M sodium phosphate, 0.1 mM EDTA, 0.30 mM sodium octyl sulfate and 5% (v/v) acetonitrile, pH 3.2. The dopamine and DOPAC amount (ng/sample) was then quantified by comparison to internal standards, with a standard curve generated with 0.1–5 ng of dopamine standard. The protein level (mg/sample) was determined with Lowry protein assays with a standard curve generated with 0–95 μg bovine serum albumin.

MPTP injection

MPTP (30 mg/kg) was injected intraperitoneally (i.p.) to SNCA TG mice with AEP WT or KO ($N = 3$, respectively), and MAO-B WT or

KO ($N = 3$, respectively) mice. MPTP was injected daily for 5 days. Mice are euthanized, and tissues are collected after 5 days from the last day of injection.

Rasagiline administration

Mice were injected with AAV-α-Syn or AAV-GFP in the right side of substantia nigra. Rasagiline (Sigma) or vehicle was administered in the drinking water to virus-injected mice for 15 weeks. Daily water intake of mice was measured as about 5.8 ml/25 g mouse before administration. The oral dose of Rasagiline was about 3 mg/kg/day.

Stereotaxic injection

AAV-GFP, AAV-α-Syn, AAV-α-Syn N103, AAV-AEP, or AAV-AEP C189S were injected into the substantia nigra of mice. 3-month-old mice of each group were anesthetized with isoflurane (Piramal Healthcare). Meloxicam (2 mg/kg) was injected subcutaneously for analgesics (Loxicom, Norbrook). Unilateral intracerebral injection of virus was performed stereotaxically at the following coordinates: anteroposterior (AP) -3.1 mm and mediolateral (ML) -1.2 mm relative to bregma, and dorsoventral (DV) -4.3 mm from the dural surface. 2 µl of viral suspension was injected into each site using 10-µl Hamilton syringe with a fixed needle at a rate of 0.25 µl/min. The needle was remained in place for 5 min after the viral suspension was completely injected. The needle was removed slowly (over 2 min). The mice were placed on heating pad until it began to recover from the anesthesia.

Behavioral test

Loss of motor function due to DAergic neurodegeneration was tested 15 weeks following the vector injection. Behavioral test included the rotarod test, cylinder test, and amphetamine-induced rotation. For the rotarod test, mice were trained for 3 sequential days on the rotarod. Each daily practice session consisted of placing the subject on the rotarod (San Diego Instruments) at a slow rotational speed (5 rpm) for a maximum of 10 min. Mice were given three test trials on the test day. The rotational speed of rotarod was modulated from 0 rpm to a maximum 40 rpm. It was gradually increased during the trial at a rate of 0.1 rpm/s. Latency to fall down from the accelerating rotarod, as well as the rotational speed, was the primary dependent variable. For the cylinder test, mice were placed individually inside a glass cylinder (12 cm diameter, 22 cm height) and video-recorded. Video files were examined by an observer blinded to the animal's treatment. Between 20 and 30 wall touches per animal (contacts with fully extended digits executed with the forelimb ipsilateral and contralateral to the lesion) were counted. For the amphetamine-induced rotation test, d-amphetamine (free base, 2 mg/kg in saline, Sigma) was injected i.p. The number of completed ipsilateral or contralateral circles was quantified.

Quantification and statistical analysis

TH immunoreactivity in the substantia nigra and striatum was estimated using fluorescence intensity quantified using ImageJ software. For each animal, three consecutive sections of the substantia nigra and striatum were analyzed. The values of fluorescence intensity were calculated average from each group ($N = 3$, each group). The conditions of the analysis were blinded to the investigator. Statistical analysis was performed using either Student's *t*-test (two-group comparison) or one-way ANOVA followed by LSD *post hoc* test (more than two groups), and differences with $P < 0.05$ were considered significant.

Expanded View for this article is available online.

Author contributions

KY conceived the project, designed the experiments, and wrote the manuscript. SSK designed and performed most of the experiments. EHA, ZZ, and XL prepared primary neurons and assisted with animal experiments. FPM and IMS provided clones and packaged viral vectors. SD and PMI performed HPLC experiments. SSK, ZZ, FPM, PMI, and XC assisted with data interpretation and critically read the manuscript.

Conflict of interest

The authors declare that they have no conflict of interest.

References

Anderson DG, Mariappan SV, Buettner GR, Doorn JA (2011) Oxidation of 3,4-dihydroxyphenylacetaldehyde, a toxic dopaminergic metabolite, to a semiquinone radical and an ortho-quinone. *J Biol Chem* 286: 26978–26986

Bensky MJ, Sandoval IM, Manfredsson FP (2016) Continuous collection of adeno-associated virus from producer cell medium significantly increases total viral yield. *Hum Gene Ther Methods* 27: 32–45

Burke WJ (2003) 3,4-dihydroxyphenylacetaldehyde: a potential target for neuroprotective therapy in Parkinson's disease. *Curr Drug Targets CNS Neurol Disord* 2: 143–148

Burke WJ, Li SW, Williams EA, Nonneman R, Zahm DS (2003) 3,4-Dihydroxyphenylacetaldehyde is the toxic dopamine metabolite *in vivo*: implications for Parkinson's disease pathogenesis. *Brain Res* 989: 205–213

Burke WJ, Li SW, Chung HD, Ruggiero DA, Kristal BS, Johnson EM, Lampe P, Kumar VB, Franko M, Williams EA, Zahm DS (2004) Neurotoxicity of MAO metabolites of catecholamine neurotransmitters: role in neurodegenerative diseases. *Neurotoxicology* 25: 101–115

Burke WJ, Kumar VB, Pandey N, Panneton WM, Gan Q, Franko MW, O'Dell M, Li SW, Pan Y, Chung HD, Galvin JE (2008) Aggregation of alpha-synuclein by DOPAL, the monoamine oxidase metabolite of dopamine. *Acta Neuropathol* 115: 193–203

Chau KY, Cooper JM, Schapira AH (2010) Rasagiline protects against alpha-synuclein induced sensitivity to oxidative stress in dopaminergic cells. *Neurochem Int* 57: 525–529

Chen JF, Steyn S, Staal R, Petzer JP, Xu K, Van Der Schyf CJ, Castagnoli K, Sonsalla PK, Castagnoli N Jr, Schwarzschild MA (2002) 8-(3-Chlorostyryl) caffeine may attenuate MPTP neurotoxicity through dual actions of monoamine oxidase inhibition and A2A receptor antagonism. *J Biol Chem* 277: 36040–36044

Chu Y, Kordower JH (2007) Age-associated increases of alpha-synuclein in monkeys and humans are associated with nigrostriatal dopamine depletion: is this the target for Parkinson's disease? *Neurobiol Dis* 25: 134−149

Conway KA, Rochet JC, Bieganski RM, Lansbury PT Jr (2001) Kinetic stabilization of the alpha-synuclein protofibril by a dopamine-alpha-synuclein adduct. *Science* 294: 1346−1349

Edmondson DE, Binda C, Mattevi A (2007) Structural insights into the mechanism of amine oxidation by monoamine oxidases A and B. *Arch Biochem Biophys* 464: 269−276

Galter D, Buervenich S, Carmine A, Anvret M, Olson L (2003) ALDH1 mRNA: presence in human dopamine neurons and decreases in substantia nigra in Parkinson's disease and in the ventral tegmental area in schizophrenia. *Neurobiol Dis* 14: 637−647

Goldstein DS, Kopin IJ, Sharabi Y (2014) Catecholamine autotoxicity. Implications for pharmacology and therapeutics of Parkinson disease and related disorders. *Pharmacol Ther* 144: 268−282

Gomez-Santos C, Barrachina M, Gimenez-Xavier P, Dalfo E, Ferrer I, Ambrosio S (2005) Induction of C/EBP beta and GADD153 expression by dopamine in human neuroblastoma cells. Relationship with alpha-synuclein increase and cell damage. *Brain Res Bull* 65: 87−95

Grimm J, Mueller A, Hefti F, Rosenthal A (2004) Molecular basis for catecholaminergic neuron diversity. *Proc Natl Acad Sci USA* 101: 13891−13896

Grimsby J, Toth M, Chen K, Kumazawa T, Klaidman L, Adams JD, Karoum F, Gal J, Shih JC (1997) Increased stress response and beta-phenylethylamine in MAOB-deficient mice. *Nat Genet* 17: 206−210

Hasegawa T, Matsuzaki-Kobayashi M, Takeda A, Sugeno N, Kikuchi A, Furukawa K, Perry G, Smith MA, Itoyama Y (2006) Alpha-synuclein facilitates the toxicity of oxidized catechol metabolites: implications for selective neurodegeneration in Parkinson's disease. *FEBS Lett* 580: 2147−2152

Heikkila RE, Hess A, Duvoisin RC (1984) Dopaminergic neurotoxicity of 1-methyl-4-phenyl-1,2,5,6-tetrahydropyridine in mice. *Science* 224: 1451−1453

Janezic S, Threlfell S, Dodson PD, Dowie MJ, Taylor TN, Potgieter D, Parkkinen L, Senior SL, Anwar S, Ryan B, Deltheil T, Kosillo P, Cioroch M, Wagner K, Ansorge O, Bannerman DM, Bolam JP, Magill PJ, Cragg SJ, Wade-Martins R (2013) Deficits in dopaminergic transmission precede neuron loss and dysfunction in a new Parkinson model. *Proc Natl Acad Sci USA* 110: E4016−E4025

Javitch JA, D'Amato RJ, Strittmatter SM, Snyder SH (1985) Parkinsonism-inducing neurotoxin, N-methyl-4-phenyl-1,2,3,6 -tetrahydropyridine: uptake of the metabolite N-methyl-4-phenylpyridine by dopamine neurons explains selective toxicity. *Proc Natl Acad Sci USA* 82: 2173−2177

Jellinger KA (2004) Lewy body-related alpha-synucleinopathy in the aged human brain. *J Neural Transm (Vienna)* 111: 1219−1235

van Kasteren SI, Berlin I, Colbert JD, Keane D, Ovaa H, Watts C (2011) A multifunctional protease inhibitor to regulate endolysosomal function. *ACS Chem Biol* 6: 1198−1204

Klivenyi P, Siwek D, Gardian G, Yang L, Starkov A, Cleren C, Ferrante RJ, Kowall NW, Abeliovich A, Beal MF (2006) Mice lacking alpha-synuclein are resistant to mitochondrial toxins. *Neurobiol Dis* 21: 541−548

Koppula S, Kumar H, Kim IS, Choi DK (2012) Reactive oxygen species and inhibitors of inflammatory enzymes, NADPH oxidase, and iNOS in experimental models of Parkinson's disease. *Mediators Inflamm* 2012: 823902

Kowall NW, Hantraye P, Brouillet E, Beal MF, McKee AC, Ferrante RJ (2000) MPTP induces alpha-synuclein aggregation in the substantia nigra of baboons. *NeuroReport* 11: 211−213

Kruger R, Kuhn W, Muller T, Woitalla D, Graeber M, Kosel S, Przuntek H, Epplen JT, Schols L, Riess O (1998) Ala30Pro mutation in the gene encoding alpha-synuclein in Parkinson's disease. *Nat Genet* 18: 106−108

Lamensdorf I, Eisenhofer G, Harvey-White J, Hayakawa Y, Kirk K, Kopin IJ (2000) Metabolic stress in PC12 cells induces the formation of the endogenous dopaminergic neurotoxin, 3,4-dihydroxyphenylacetaldehyde. *J Neurosci Res* 60: 552−558

Langston JW, Ballard PA Jr (1983) Parkinson's disease in a chemist working with 1-methyl-4-phenyl-1,2,5,6-tetrahydropyridine. *N Engl J Med* 309: 310

Lee VM, Trojanowski JQ (2006) Mechanisms of Parkinson's disease linked to pathological alpha-synuclein: new targets for drug discovery. *Neuron* 52: 33−38

Li W, West N, Colla E, Pletnikova O, Troncoso JC, Marsh L, Dawson TM, Jakala P, Hartmann T, Price DL, Lee MK (2005) Aggregation promoting C-terminal truncation of alpha-synuclein is a normal cellular process and is enhanced by the familial Parkinson's disease-linked mutations. *Proc Natl Acad Sci USA* 102: 2162−2167

Lieu CA, Chinta SJ, Rane A, Andersen JK (2013) Age-related behavioral phenotype of an astrocytic monoamine oxidase-B transgenic mouse model of Parkinson's disease. *PLoS ONE* 8: e54200

Liu Z, Jang SW, Liu X, Cheng D, Peng J, Yepes M, Li XJ, Matthews S, Watts C, Asano M, Hara-Nishimura I, Luo HR, Ye K (2008) Neuroprotective actions of PIKE-L by inhibition of SET proteolytic degradation by asparagine endopeptidase. *Mol Cell* 29: 665−678

Mahy N, Andres N, Andrade C, Saura J (2000) Age-related changes of MAO-A and -B distribution in human and mouse brain. *Neurobiology (Bp)* 8: 47−54

Mallajosyula JK, Kaur D, Chinta SJ, Rajagopalan S, Rane A, Nicholls DG, Di Monte DA, Macarthur H, Andersen JK (2008) MAO-B elevation in mouse brain astrocytes results in Parkinson's pathology. *PLoS ONE* 3: e1616

Mandel S, Weinreb O, Amit T, Youdim MB (2005) Mechanism of neuroprotective action of the anti-Parkinson drug rasagiline and its derivatives. *Brain Res Brain Res Rev* 48: 379−387

Maruyama W, Weinstock M, Youdim MB, Nagai M, Naoi M (2003) Anti-apoptotic action of anti-Alzheimer drug, TV3326 [(N-propargyl)-(3R)-aminoindan-5-yl]-ethyl methyl carbamate, a novel cholinesterase-monoamine oxidase inhibitor. *Neurosci Lett* 341: 233−236

Murray IV, Giasson BI, Quinn SM, Koppaka V, Axelsen PH, Ischiropoulos H, Trojanowski JQ, Lee VM (2003) Role of alpha-synuclein carboxy-terminus on fibril formation *in vitro*. *Biochemistry* 42: 8530−8540

Norris EH, Giasson BI, Ischiropoulos H, Lee VM (2003) Effects of oxidative and nitrative challenges on alpha-synuclein fibrillogenesis involve distinct mechanisms of protein modifications. *J Biol Chem* 278: 27230−27240

Panneton WM, Kumar VB, Gan Q, Burke WJ, Galvin JE (2010) The neurotoxicity of DOPAL: behavioral and stereological evidence for its role in Parkinson disease pathogenesis. *PLoS ONE* 5: e15251

Polymeropoulos MH, Lavedan C, Leroy E, Ide SE, Dehejia A, Dutra A, Pike B, Root H, Rubenstein J, Boyer R, Stenroos ES, Chandrasekharappa S, Athanassiadou A, Papapetropoulos T, Johnson WG, Lazzarini AM, Duvoisin RC, Di Iorio G, Golbe LI, Nussbaum RL (1997) Mutation in the alpha-synuclein gene identified in families with Parkinson's disease. *Science* 276: 2045−2047

Przedborski S, Jackson-Lewis V (1998) Mechanisms of MPTP toxicity. *Mov Disord* 13(Suppl 1): 35−38

Ramsay RR, Singer TP (1986) Energy-dependent uptake of N-methyl-4-phenylpyridinium, the neurotoxic metabolite of 1-methyl-4-phenyl-1,2,3,6-tetrahydropyridine, by mitochondria. *J Biol Chem* 261: 7585−7587

Riederer P, Jellinger K (1983) Neurochemical insights into monoamine oxidase inhibitors, with special reference to deprenyl (selegiline). *Acta Neurol Scand Suppl* 95: 43−55

Saura J, Richards JG, Mahy N (1994) Differential age-related changes of MAO-A and MAO-B in mouse brain and peripheral organs. *Neurobiol Aging* 15: 399−408

Schapira AH (2008) Progress in neuroprotection in Parkinson's disease. *Eur J Neurol* 15(Suppl 1): 5−13

Schapira AH, Olanow CW (2008) Drug selection and timing of initiation of treatment in early Parkinson's disease. *Ann Neurol* 64(Suppl 2): S47−S55

Schluter OM, Fornai F, Alessandri MG, Takamori S, Geppert M, Jahn R, Sudhof TC (2003) Role of alpha-synuclein in 1-methyl-4-phenyl-1,2,3,6-tetrahydropyridine-induced parkinsonism in mice. *Neuroscience* 118: 985−1002

Shih JC (2004) Cloning, after cloning, knock-out mice, and physiological functions of MAO A and B. *Neurotoxicology* 25: 21−30

Siddiqui A, Mallajosyula JK, Rane A, Andersen JK (2011) Ability to delay neuropathological events associated with astrocytic MAO-B increase in a Parkinsonian mouse model: implications for early intervention on disease progression. *Neurobiol Dis* 43: 527−532

Thomas B, Mandir AS, West N, Liu Y, Andrabi SA, Stirling W, Dawson VL, Dawson TM, Lee MK (2011) Resistance to MPTP-neurotoxicity in alpha-synuclein knockout mice is complemented by human alpha-synuclein and associated with increased beta-synuclein and Akt activation. *PLoS ONE* 6: e16706

Vila M, Vukosavic S, Jackson-Lewis V, Neystat M, Jakowec M, Przedborski S (2000) Alpha-synuclein up-regulation in substantia nigra dopaminergic neurons following administration of the parkinsonian toxin MPTP. *J Neurochem* 74: 721−729

Wakamatsu M, Ishii A, Iwata S, Sakagami J, Ukai Y, Ono M, Kanbe D, Muramatsu S, Kobayashi K, Iwatsubo T, Yoshimoto M (2008) Selective loss

of nigral dopamine neurons induced by overexpression of truncated human alpha-synuclein in mice. *Neurobiol Aging* 29: 574−585

Wei Q, Yeung M, Jurma OP, Andersen JK (1996) Genetic elevation of monoamine oxidase levels in dopaminergic PC12 cells results in increased free radical damage and sensitivity to MPTP. *J Neurosci Res* 46: 666−673

Wei Q, Jurma OP, Andersen JK (1997) Increased expression of monoamine oxidase-B results in enhanced neurite degeneration in methamphetamine-treated PC12 cells. *J Neurosci Res* 50: 618−626

Youdim MB, Weinstock M (2001) Molecular basis of neuroprotective activities of rasagiline and the anti-Alzheimer drug TV3326 [(N-propargyl-(3R) aminoindan-5-YL)-ethyl methyl carbamate]. *Cell Mol Neurobiol* 21: 555−573

Youdim MB, Gross A, Finberg JP (2001) Rasagiline [N-propargyl-1R(+)-aminoindan], a selective and potent inhibitor of mitochondrial monoamine oxidase B. *Br J Pharmacol* 132: 500−506

Youdim MB, Fridkin M, Zheng H (2005) Bifunctional drug derivatives of MAO-B inhibitor rasagiline and iron chelator VK-28 as a more effective approach to treatment of brain ageing and ageing neurodegenerative diseases. *Mech Ageing Dev* 126: 317−326

Zhang Z, Song M, Liu X, Kang SS, Kwon IS, Duong DM, Seyfried NT, Hu WT, Liu Z, Wang JZ, Cheng L, Sun YE, Yu SP, Levey AI, Ye K (2014) Cleavage of tau by asparagine endopeptidase mediates the neurofibrillary pathology in Alzheimer's disease. *Nat Med* 20: 1254−1262

Zhang Z, Song M, Liu X, Su Kang S, Duong DM, Seyfried NT, Cao X, Cheng L, Sun YE, Ping Yu S, Jia J, Levey AI, Ye K (2015) Delta-secretase cleaves amyloid precursor protein and regulates the pathogenesis in Alzheimer's disease. *Nat Commun* 6: 8762

Zhang Z, Kang SS, Liu X, Ahn EH, Zhang Z, He L, Iuvone PM, Duong DM, Seyfried NT, Benskey MJ, Manfredsson FP, Jin L, Sun YE, Wang JZ, Ye K (2017a) Asparagine endopeptidase cleaves alpha-synuclein and mediates pathologic activities in Parkinson's disease. *Nat Struct Mol Biol* 24: 632−642

Zhang Z, Obianyo O, Dall E, Du Y, Fu H, Liu X, Kang SS, Song M, Yu SP, Cabrele C, Schubert M, Li X, Wang JZ, Brandstetter H, Ye K (2017b) Inhibition of delta-secretase improves cognitive functions in mouse models of Alzheimer's disease. *Nat Commun* 8: 14740